Marta Teresa da Silva Gomes

Isolation of novel immunogenic protein carriers for vaccine development

October 2022

Universidade do Minho
Escola de Engenharia
Escola de Medicina

Marta Teresa da Silva Gomes

Isolation of novel immunogenic protein carriers for vaccine development

Master's Dissertation
Master's degree in Biotechnology

Work conducted under the guidance of:
Doctor Hugo Alexandre Mendes de Oliveira
Doctor Alexandra Gabriel Fraga

October 2022

Direitos de autor e condições de utilização do trabalho por terceiros

Este é um trabalho académico que pode ser utilizado por terceiros desde que respeitadas as regras e boas práticas internacionalmente aceites, no que respeita aos direitos de autor e direitos conexos.

Assim, o presente trabalho pode ser utilizado nos termos previstos na licença abaixo indicada.

Caso o utilizador necessite de permissão para poder fazer um uso do trabalho em condições não previstas no licenciamento indicado, deverá contactar o autor, através do RepositóriUM da Universidade do Minho.

Acknowledgements

Statement of Integrity

I, Marta Gomes, hereby declare having conducted this academic work with integrity. I confirm that I have not used plagiarism or any form of undue use of information or falsification of results along the process leading to its elaboration.

I further declare that I have fully acknowledged the Code of Ethical Conduct of the University of Minho.

Resumo

Os antibióticos têm sido amplamente usados no tratamento de infeções bacterianas, contudo o seu uso extensivo e indiscriminado tem levado ao aparecimento de organismos resistentes. *Acinetobacter baumannii* é uma bactéria multirresistente, regularmente encontrada em infeções nosocomiais, e foi indicada pela Organização Mundial da Saúde como prioritária no desenvolvimento de novas estratégias antimicrobianas. Dentro das alternativas, as vacinas surgem como abordagens de profilaxia. Assim, neste projeto pretende-se desenvolver uma nova pipeline para prever o potencial imunogénico de proteínas bacterianas, validar e aumentar o número de proteínas imunogénicas contra *A. baumannii*.

Neste estudo, 21 proteínas de *A. baumannii* ATCC 17978 foram selecionadas através de ferramentas de vacinologia reversa e imunoinformática. Destas, as proteínas NlpE e BamE selecionadas e comparadas com a Omp33 com imunogenicidade comprovada. Expressão heteróloga recombinante sem os péptidos de sinal N-terminais resultou em proteínas solúveis, e análise por Dicroísmo Circular confirmou o seu enrolamento correto. *In vivo*, avaliamos a resposta imune contra estas proteínas em ratinhos Balb/c, após três inoculações. Ensaios de ELISA mostraram que todas as proteínas induziram síntese de anticorpos, e análises histológicas não revelaram sinais de patogenicidade.

Adicionalmente, a compreensão dos mecanismos de virulência dos microrganismos é essencial para a evolução das terapias. Assim, surge a questão se proteínas envolvidas na virulência têm potencial imunogénico e vice-versa. Portanto, pretendeu-se também estudar o papel das proteínas Omp33, NlpE e BamE na virulência da bactéria, através da construção de mutantes de *A. baumannii* ATCC 17978 por CRISPR/Cas9. Ensaios de cinética de crescimento, formação de biofilme e sobrevivência em contato com soro humano mostraram que, apesar da menor cinética de crescimento dos mutantes, estes apresentam uma maior capacidade de formar biofilmes e não apresentam diferenças significativas na sobrevivência contra soro humano.

Em suma, confirmamos que a combinação de ferramentas computacionais pode ser usada para previsão de proteínas imunogénicas. Neste trabalho, isolamos com sucesso duas novas proteínas com potencial de serem aplicadas em vacinas contra *A. baumannii*. Relativamente ao seu papel na virulência, ensaios adicionais mais específicos deverão ser realizados.

Palavras-chave: *Acinetobacter*, CRISPR/Cas9, imunoinformática, vacinologia reversa, virulência

Abstract

Antibiotics have been successfully used to treat bacterial infections, yet its extensive and indiscriminate use has led to the appearance of resistant organisms. *Acinetobacter baumannii* is a multidrug-resistant bacterium, commonly found in nosocomial infections, which was listed by the World Health Organization as a priority in the development of new antimicrobial strategies. Among the alternatives, vaccines come as promising prophylactic approaches. Consequently, this project aims to create a new pipeline to predict the immunogenic potential of bacterial proteins, to validate and to expand the number of immunogenic proteins against *A. baumannii*.

In this study, 21 *A. baumannii* ATCC 17978 proteins were selected as candidates using reverse vaccinology and immunoinformatic tools. From these, the NlpE and BamE were selected and compared with the outer membrane proteins Omp33 with proven immunogenicity. Heterologous recombinant expression without the N-terminal signal peptides resulted in soluble proteins, and Circular Dichroism ensured their proper folding. *In vivo*, we evaluated the immune response against these proteins in Balb/c mice, following three inoculations. ELISA assays with the mice's sera showed that antibodies were synthesized against all proteins, and histology analysis revealed no signs of pathogenicity.

Moreover, understanding the microorganism's virulence factors is essential for the evolution of therapies. Thus, arises the hypothesis that virulence engaged proteins might have immunogenic potential and vice-versa. So, it was also intended to study the role of proteins Omp33, NlpE and BamE in the bacteria's virulence, by constructing single-gene deletion mutants of *A. baumannii* ATCC 17978 using CRISPR/Cas9 genome edition. Growth kinetics, biofilm formation and survival in contact with human serum assays showed that, despite the lower growth kinetics of the mutants, they have an increased ability to form biofilms and show no significant differences in survival against human serum, compared to the wild-type strain.

Overall, the results illustrate that the combination of computational tools and virulence-associated analysis can be used to anticipate the proteins' immunogenicity. Herein, we have successfully isolated two novel proteins with potential application in vaccines against *A. baumannii*. Regarding their role in virulence, more specific assays should be further performed.

Keywords: *Acinetobacter*, CRISPR/Cas9, immunoinformatics, reverse vaccinology, virulence

Table of Contents

List of Presentations

<u>Poster</u>

Gomes M, Domingues R, Fraga A, Oliveira H. 2022. Optimized identification and expression of *A. baumannii* immunogenic proteins. International conference *AcinetoVibes*, June, 2022, virtual meeting.

- Outstanding poster award

<u>Oral</u>

Gomes M, Domingues R, Fraga A, Oliveira H. 2022. Proteínas imunogénicas contra *A. baumannii*: recurso para combater multirresistência. International congress *Microbiologia 2022*, October, 2022, virtual meeting.

List of Abbreviations and Acronyms

AMPs	Antimicrobial Peptides
AMR	Antimicrobial Resistance
ANOVA	Analysis of variance
APC	Antigen Presenting Cell
apr	Apramycin
BamE	Outer Membrane Assembly Factor BamE
BLAST	Basis Local Alignment Search Tool
bp	Base Pairs
BSA	Bovine Serum Albumin
CD	Circular Dichroism
CFU	Colony Forming Units
CRISPR/Cas9	Clustered Regularly Interspaced Short Palindromic Repeat associated Nuclease 9
DNA	Deoxyribonucleic Acid
dNTP	Deoxynucleotide triphosphate
DT	Diphtheria Toxoid
Dt	Duplication Time
EC	Electrocompetent
EU	Endotoxin Units
HLA	Human Leukocyte Antigen
HP504	Hypothetical Protein 504
ICVS	Health and Life Sciences Institute
IEDB	Immune Epitope Database
IEDB – AR	IEDB – Analysis Resource
IPTG	β-D-1-thiogalactopyranoside
LB	Luria Broth
LBA	Luria Broth Agar
LP	Lipocalin Family Protein
LPS	Lipopolysaccharide
kDa	Kilodalton
km	Kanamycin
MHC	Major Histocompatibility Complex
MlaD	Maintenance Protein MlaD
mRNA	Messenger Ribonucleic Acid

N-terminal	Amino-terminal
Ni²⁺-NTA	Nickel-charged affinity resin
NlpE	Copper Resistance Protein NlpE
OD	Optical Density
Omp	Outer Membrane Protein
Omp33	Outer Membrane Protein 33-36
OmpA	Outer Membrane Protein A
OmpA2	OmpA Family protein
OmpW	Outer Membrane Protein W
PBS	Phosphate-Buffered Saline
PCR	Polymerase Chain Reaction
PP	Putative porin protein
PRRs	Pattern Recognition Receptors
rpm	Rotations per minute
RT	Room Temperature
RNA	Ribonucleic Acid
RT	Room Temperature
SDS-PAGE	Sodium Dodecyl Sulphate Polyacrylamide Gel Electrophoresis
SOC	Super Optimal Broth
TCR	T-cell Receptors
TSB	Tryptic Soy Broth
TSA	Tryptic Soy Agar
TT	Tetanus Toxoid
WT	Wild-Type
μ	Exponential Growth Rate

List of Figures

List of Tables

CHAPTER 1

General Introduction

1.1. Impact of drug-resistant bacterial infections

Bacterial infections have always had a great impact on human health. Antibiotics are substances produced by microorganisms with antagonistic effects on the growth of other microbes and have been used to successfully treat and prevent infections in humans [1]. Beyond the treatment of human infections, antibiotics are widely used in agriculture, to treat animals and promote their growth, and on crops to improve their development. Despite their success, their indiscriminate use has allowed bacteria to evolve to become less prone or even resistant to many antibiotics, putting these therapies at risk [2]. The unprecedent rise of antimicrobial resistance (AMR) in bacteria is one of the greatest threats to humankind of the new millennium, as pointed by both the Infectious Diseases Society of America and the European Society of Clinical Microbiology and Infectious Diseases. Nosocomial infections, which occur during hospitalization, are highly associated with the dissemination of resistant bacteria[3]. The ESKAPE pathogens (an acronym for *Enterococcus faecium*, *Staphylococcus aureus*, *Klebsiella pneumoniae*, *Acinetobacter baumannii*, *Pseudomonas aeruginosa* and *Enterobacter spp.*) are a group of multidrug-resistant pathogens, causers of life-threatening infections. Within these, the World Health Organization listed *A. baumannii* as a priority for the development of new antimicrobial strategies, since some strains are already resistant to several antimicrobial drugs, including some last-line antibiotics.

AMR bacterial infections have increased dramatically over the past few years, and it is estimated that these kill 700,000 individuals annually. Due to the globalization of resistance and the lack of development of new classes of antibiotics, it is possible that, in the next five years, not only will there be a global inefficacy of currently used antibiotics, but AMR infections will kill up to an estimated 10 million people every year [4,5]. Furthermore, AMR infections have associated costs, causing economic losses of €1.5 billion every year in the European Union and US$5 billion in the United States of America [6]. Additionally, antibiotic development is no longer seen as an economically wise investment for the pharmaceutical industry since they are not as profitable as drugs that treat chronic conditions. Besides that, when new antibiotic agents are approved, these are viewed as a last line of defence, to delay the arise of bacterial resistance [2,5]. Therefore, there is a need for the development of new antimicrobial strategies.

Acinetobacter baumannii: Virulence factors and resistance

A. baumannii is one of the most relevant _Acinetobacter_ species, at a clinical level and is involved in the majority of nosocomial infections [7]. In general, this genus is characterized as small pleomorphic, Gram-negative coccobacillus, strictly aerobic, catalase- and oxidase-positive, nonfermenting and nonmotile [8,9]. The characteristics of resistance, even to dry conditions, the ability to grow across a variety of temperatures, pH, and nutrient levels, and even the capacity to survive up to five months on surfaces, provides _A. baumannii_ with a great ability to survive and spread as a nosocomial agent, especially in debilitated patients hospitalized in intensive units [6]. In the last years there has been a significant increase in the number of _A. baumannii_ infections in the respiratory tract, blood vessels, urinary system, skin, soft tissues, and in the central nervous system, especially in patients who needed ventilation or other medical devices [8].

A. baumannii has proved to be an extremely problematic nosocomial pathogen. In addition, this bacterium has multiple survival mechanisms upon different environmental conditions and has a high ability to acquire or upregulate numerous resistance factors, making it a major AMR pathogen and putting current antimicrobial therapies at risk. Despite several studies on _A. baumannii_, it has not yet been possible to identify the virulence factors responsible for the high occurrence of this bacterium at the clinical level. Nevertheless, in general, the presence of porins, capsular polysaccharides and lipopolysaccharides (LPS); the production of hydrolytic enzymes and of siderophores; and the toxin secretion can be identified as virulence factors [7,10,11]. The presence of the outer membrane protein A, or Omp38, is also pointed as a virulence factor, since it induces apoptosis in epithelial cells [6,11].

A. baumannii's increased resistance to antibiotics, such as β-lactam antibiotics, first and second generation cephalosporins and aminopenicillins, as well as the appearance of strains resistant to all current antibiotics, is very troubling [7]. Additionally, although the resistant bacteria started to be treated with carbapenems, the emergence and spread of strains also resistant to this drug has limited its effectiveness. Moreover, strains resistant to colistin have also emerged, mostly attributed to changes in the structure of the LPS and to plasmid-carrying resistance genes [10]. As a Gram-negative bacteria, _A. baumannii_ has, intrinsically, higher chances to resist antibiotics' action due the presence of the outer membrane which, together with the active efflux pump system and the low quantity expression of small outer membrane porins, decreases the permeability to

antibiotics [6]. Currently, the treatment of infections by *A. baumannii* is limited due its ability to acquire resistance and to adapt to environmental changes.

1.2. Alternative antimicrobial strategies

To change the current AMR situation, effective actions must be taken to control the spread of AMR microorganisms. There are several emerging therapies that have been developed, namely antibody and antivirulence-strategies. While therapeutic antibodies are used as prophylactics or even as therapies for bacterial infection, antivirulence strategies are applied to attenuate the virulence of pathogens by removing virulence factors (e.g., adhesins, capsules) leaving the pathogen more vulnerable to the host immunity. Other more well-established antimicrobial strategies, such as bacteriophages, antibacterial peptides and vaccines are discussed next.

Bacteriophages

Bacteriophages (or phages) are viruses that only infect bacterial cells and are one of the most abundant entities in Nature. They are easily isolated and able to control pathogens, without affecting commensal bacteria or eukaryotic cells, due their high specificity to the host. Phage therapy is therefore seen as an alternative strategy to antibiotics [12,13]. However, to apply this kind of therapy, it is necessary, at a first stage, to identify the pathogenic agent and then, select the adequate phage. Also, since phage particles have some proteins with unknown functions, they can transfer harmful genes from one bacterium to another (e.g., antibiotic-resistant genes or toxins). Moreover, it is necessary to know the best frequency of administration, dose, and regime to optimize these phage-based therapies [5,14].

Although there are still several constrains that counteract the implementation of phage therapy, it has already been applied both in animal models and patients. According to the literature, the best source to isolate *A. baumannii* phages are hospital sewages and wastewaters[13,15]. Several studies showed favourable clinical results of phage cocktails against *A. baumannii* infections, as well in cases of infection by multi-drug resistant strains of *A. baumannii* [14,16–19]. One example is the case of Thomas Patterson, the first known person in the United States to successfully undergo intravenous phage therapy. After being infected with a MDR *A. baumannii* strain, in 2016, Patterson's health was rapidly declining, leading to a coma. However, after being administered a

high specific phage cocktail against *A. baumannii*, his clinical condition quickly changed, and he was able to fully recover within weeks [18].

Phage-derived proteins have also emerged as another source of antimicrobial agents. The most widely known example are the endolysins. These are enzymes produced by phages during the last stage of viral infection, to digest the bacterial cell wall and to lyse the cells. Several endolysins have been heterologously expressed as recombinant enzymes with high therapeutic efficacy in controlling bacterial infections in both *in vitro* and *in vivo* pre-clinical tests against drug-resistant pathogens, including *A. baumannii* [20]. Additionally, there has been reported synergism both between different endolysins, and with antibiotics. Another example of phage-derived proteins are depolymerases. These are receptor-binding proteins, carried by phages, that bind to bacterial receptors and are able to depolymerize the capsule, which leads to further infection by the phage [21]. The capsule's cleavage aids the immune system to fight the bacterial infection, hence, the use of phage-derived polymerases as potential therapeutic agents [22]. This premise has been broadly tested *in vitro*, through recombinant expression of the depolymerases and administration to the bacterial culture, with encouraging results [22–24].

Antimicrobial peptides

Antimicrobial peptides (AMPs) are polypeptides that constitute a defence strategy of both animals and plants against bacteria, fungi, and viruses [25]. Not only do these peptides stimulate the accumulation of immune cells at the site of infection, but they also neutralize endotoxins, accelerate wound repair, stimulate angiogenesis, behave as immunomodulators, and have anti-inflammatory properties. Therefore, AMPs may be applied with or as antimicrobial agents. In addition, AMPs have a wide action spectrum, acting quickly even in extremely low amounts, and there is a reduced chance of bacteria developing resistance to these peptides. Nevertheless, they may lose their activity either by pH variations or due the presence of proteases. They can also have toxic effects and may induce sensibility or even allergic reactions, after several applications [25]. Besides, they are still to be studied from the perspective of pharmacokinetics, pharmacodynamics, and toxicity [5]. From another viewpoint, bacteriocins, a subgroup of AMPs produced by bacteria as defence mechanism, inhibiting the growth of bacteria either from the same specie or the same genus, and

may be used in the pharmaceutical industry. Cec4, SMAP-29 or TP4 are promising AMP examples against *A. baumannii* [26,27].

Vaccines

Vaccines are prophylactic strategies against infections. They are administered to healthy individuals and, like other drugs, may have adverse reactions, even though mostly acute and transient, and rarely causing hypersensitivity [28]. There are two categories of vaccines: active vaccines and passive vaccines, which have different types of approaches. While active vaccines stimulate the host's own immune response and leads to the production of antibodies, passive vaccines consist in the administration of antibodies to either neutralize an antigen or to bind to a human cellular antigen [29].

Passive vaccines refer to preparations of monoclonal or polyclonal antibodies and are used when there is a necessity for an immediate immunological activity, either to prevent or to treat an infectious disease, cancer, or other non-infectious illnesses [30]. Although they are of quick action, these vaccines provide a brief protection, granting immunity only for several weeks to 3/4 months due the eventual catabolization of the antibodies [29,30]. Because of this, some patients may require a new administration of the vaccine to ensure the proper recovery.

Active vaccines should incite a life-long immunity with minimal side effects following administration. Within active vaccines, there are three main types: 1) live vaccines; 2) nucleic acid-based vaccines and 3) subunit vaccines [31].

In general, live vaccines consist of bacteria that, even though are weakened and, ideally, do not provoke an infection, elicit a very similar immune response to that induced by natural infection [32]. However, the effective attenuation of some bacterial species has been difficult to achieve [31], delaying the development of such vaccines.

Nucleic acid-based vaccines use DNA, encoding a vaccine antigen, cloned into a delivery plasmid or the direct injection of messenger RNA (mRNA) [32]. Nucleic acid-based vaccines are formulated so that the genetic material is translocated to the host cell, to promote the synthesis and excretion of the pathogen protein, and thus, replicate the natural infection and induce both humoral and cell-mediated immune responses [33,34]. By its turn, mRNA-based vaccines comprise

mRNA that encodes a pathogen antigen [33]. This kind of vaccine has been gaining increased interest with the current outbreak of Sars-Cov-2, being now administered as prophylactics for Covid-19. Additionally, there is no risk of infection when these vaccines are administered, since there is no live pathogen [32].

Subunit vaccines use a piece of the microorganism to create a strong immune response directed to key parts of the microbe. They can be subcategorized as protein-based, glycan-based, or conjugated protein-glycan vaccines. As glycans are considered weak immunogens, they are often linked to highly immunogenic proteins. Next, we address protein-based and conjugated vaccines in more detail, for which immunogenic proteins are crucial to use.

Subunit vaccines

Subunit vaccines have some advantages over live vaccines because of the numerous techniques available to develop them. As mentioned, these vaccines use antigens detected as foreign to humans and, consequently, has the potential to elicit an immune response [35]. However, these vaccines tend to require several administrations to obtain the desired immunity, or may even need adjuvants that supplement their action [31].

In protein-based vaccines, the genetic sequence coding for the desired antigen is identified and then expressed in a recombinant host cell. The synthesized protein is then purified and administered to animals to achieve polyclonal antibodies [31]. These vaccines have considerable potential because of their low toxicity and high applicability. Peptide-based vaccines go further since they contain only epitopes, regions of the antigen recognized by lymphocyte receptors and by antibodies, that are capable of inducing a positive and efficient immune response [36]. However, the main problem dwells in identifying the epitope region when the protein is not well characterized and its 3D structure not known. As a rule, vaccines have an antigen, the target of the immune response, and an adjuvant, to enhance an immune response to the antigen. For subunit vaccines, these adjuvants have been based on the definition of ''danger signal'', that is, conserved molecular regions that indicate the presence of dangerous microorganisms, which are recognized by pattern recognition receptors (PRRs) of the innate immune response cells [37]. There are few examples in the literature using protein-based subunit vaccines to target *A. baumannii*, which are illustrated in **Table 1**.

Table 1 – Immunogenic proteins pointed by literature. NA – not available

Immunogenic protein	Accession nº	Host	Accession nº	Ref
Putative exported protein (OmpK)	WP_001176274	*A. baumannii*	NC_010410	[38]
Putative long-chain fatty acid transport protein (Ompp1)	WP_000768265	*A. baumannii*	NC_010410	[38]
FKBP-type 22kD peptidyL-prolyl cis-trans isomerase (FKIB)	WP_000724221	*A. baumannii*	NC_010410	[38]
Outer membrane protein assembly factor (BamA)	WP_001170994	*A. baumannii*	NC_010410	[39]
Phospholipase D protein	ABO13392	*A. baumannii*	NC_009085	[40]
Outer membrane protein A (OmpA)	WP_011860175	*A. baumannii*	NC_009085	[41]
Outer membrane protein assembly factor (Oma87)	WP_002016574	*A. baumannii*	NC_010410	[42]
Membrane transporter (Ata)	A3M3H0	*A. baumannii*	NC_009085	[43]
Biofilm associated protein (Bap)	KR080550	*A. baumannii*	NA	[44]
Outer membrane protein 33-36 (Omp33)	WP_218655558	*A. baumannii*	NC_009085	[45]
PcTPRs1	KFC03078	*A. baumannii*	NZ_MJHA00000000	[46]

Conjugated vaccines have their immunogenic potential enhanced, to confer a rapid and effective impact against diseases caused by encapsulated bacteria [47]. These vaccines present epitopes that lead to the activation of T cells and, consequently, to a greater response with the generation of memory cells. Glycoconjugate vaccines are composed by a polysaccharide linked covalently to proteins. This conjugation provides the T-cell epitopes that are necessary in the germinal centres for affinity maturation of polysaccharide specific B-cells [48]. Additionally, it is also proposed that carbohydrate antigens do not bind to major histocompatibility complex (MHC) class II in their pure form, and consequently are not effectively presented to T cells. But, when combined with a protein carrier, a processed carbohydrate epitope is formed in the antigen presenting cells' (APCs') endolysosomes [47]. Thus, by binding the peptide region to MHCII, the carbohydrate section is shown on the surfaces of the APCs. The immune response will be further described later on.

Currently, licensed glycoconjugate vaccines include five carrier proteins: toxoids from diphtheria (DT) and tetanus (TT), that were initially selected as carriers due their safety; CRM$_{197}$, a

non-toxic mutant of diphtheria toxin; outer membrane protein complex (OMPC) from *Neisseria meningitidis* serogroup B; and protein D, from a non-typeable *Haemophilus influenzae* [47,49]. Of these, only three (DT, TT and CRM197) have been used in the majority of commercial conjugate vaccines. However, despite proven to be safe and effective, these three immunogens are differentiated by inherent manufacturing requirements and challenges. TT and DT require detoxification before polysaccharide conjugation using formaldehyde treatment, while the amino acid substitution in CRM197 renders the protein nontoxic and therefore does not require formaldehyde treatment, making it more advantageous to manufacture than TT or DT. Production of CRM197 is stalled, however, by the strict growth requirements of the traditional expression system (*Corynebacterium diphtheriae*) and generally lower expression yields compared to other expression systems.

1.3. The Immune System

The immune system is a line of defence against pathogens and general foreign organisms or molecules [50]. Most cells from the immune system are produced during haematopoiesis in the bone marrow and some go through processes of modification and maturation in lymphoid organs, before being released into the bloodstream. These cells have membrane proteins that act as receptors, which can bind to ligands, such as soluble molecules like cytokines or pathogen-associated molecular patterns [51]. These cells can detect changes through their receptors and modify the genetic regulation in order to react [51].

A healthy immune system must have the ability to distinguish what is exogenous from what is endogenous, and be able to adapt, flexibly, to the surrounding changes in order to recognize and act accordingly against an infection. During infection, pathogenic organisms can evade the physical and chemical barriers of the host, such as the skin, mucous, and secretions, through strategies intrinsic to each pathogen. The immune system can be divided into innate, an unspecific defence mechanism, and into adaptive immune system, which is characterized by its memory and high specificity to targeted antigens [52].

Innate immunity

The innate immune system is the very first line of defence against both infection and self-damage and is responsible for the inflammatory reaction [52,53]. It uses different receptors to perceive the environment, and targets conserved elements shared by several pathogens, triggering an inflammatory response shortly after the infection [50]. In general, the innate immune system comprises several tissues and cells, whether of hematopoietic origin or not. Within the hematopoietic cells, macrophages/monocytes, mast cells, neutrophils, eosinophils, and dendritic cells stand out [54]. In turn, non-hematopoietic elements are the first barrier of defence and include the skin and epithelial cells, that cover the gastrointestinal, genitourinary, and respiratory tracts [50,53,54]. Within the hematopoietic cells, phagocytes are crucial to the immune response since they are able to recognise potentially harmful elements. The recognition of the targeted conserved elements is enabled by pattern recognition receptors (PRR), mostly expressed by dendritic cells and macrophages, since they recognize conserved structures from microbes or viruses, called

pathogen associated molecular patterns [55]. Phagocytes will endocytose the foreign element, with the final goal of not only destroying the ingested pathogen but also breaking up its proteins into short amino acid chains, which will be loaded on a Major Histocompatibility Complex (MHC) molecule. It is possible to identify two classes of MHC, depending on whether antigens are produced intracellularly (nucleated cells) – MHC class I – or have been acquired extracellularly (APCs) – MHC class II [51]. Macrophages and dendritic cells, also known as APC, will then migrate to the nearest lymph node to present the antigen to a specific T cell, through MHC-TCR (T cell receptor) interaction, and convey information of the invading pathogen, ultimately bridging innate and adaptive immunity. Hence, the innate immune response is essential to trigger the adaptive response.

Adaptive immunity

Adaptive immunity can be activated through a signal pattern which includes the antigen, co-stimulators, inflammatory cytokines, and also, according to some studies, through commensal-derived metabolites, and tissue specific parameters [55].

T-cell response

When an individual develops an infection, the antigens of the pathogen are presented by the MHC-antigen complexes on the surface of the APCs and end up being recognized by specific TCRs, which will lead to the activation and clonal expansion of antigen-specific T-cells [51]. However, T cell reactivity depends on the way proteins are processed into peptides and presented as antigens, and their binding with the MHC class I or II[55].

There are different types of T-cells, the most common being CD4+ T-cells and CD8+ T-cells, which are effector cells for cell-mediated immunity. CD8+ T-cells (cytotoxic T-cells) are activated by the interaction with MHC class I and then migrate into the circulation. In turn, CD4+ T-cells (helper T-cells) interact with MHC class II, and produce cytokines, leading to the initiation of an immune response from other cells of the immune system, such as the potentiation of the microbicidal mechanism of macrophages and the activation of B-cells to produce immunoglobulins (antibodies), as shown in **Figure 1** [51,55,56]. There are different subtypes of CD4+ T-cells, each with an unique

function, which are defined based on their cytokine profile and lineage-specific transcription factors [56,57]. Hence, CD4+ T-cells can be differentiated into effector T-cells or regulatory T-cells. Effector T-cells can be further distinguished into T helper cells, specifically T_H1, T_H2, and T_H17, among others [57]. CD4+ T_H1 T-cells are important for the activation of a cell mediated immune response, through the production of the effector cytokines IFN-γ and IL-2, that are involved in maximizing the killing efficacy of macrophages, in causing increased expression of antigen-MHCII complexes in APCs and also in promoting the production of the opsonizing antibody IgG by B-cells. On the other hand, CD4+ T_H2 T cells are important in humoral mediated immune responses for fighting helminth infections (caused by parasitic worms) and participating in allergic reactions. T_H2 effector cytokines include IL-4, IL-5, and IL-13, among others, and are responsible for stimulating B-cell activation and proliferation into plasma cells and long-lived memory B-cells; and inducing B-cell antibody class switching into neutralizing antibody production IgG, IgM and IgA as well as IgE antibodies). CD4+ T_H17 T cells are a subset of T helper cells that are characterized by the production of the pro-inflammatory cytokine IL-17, vital in the immunity of mucous membranes, combating extracellular bacteria and fungi [56].
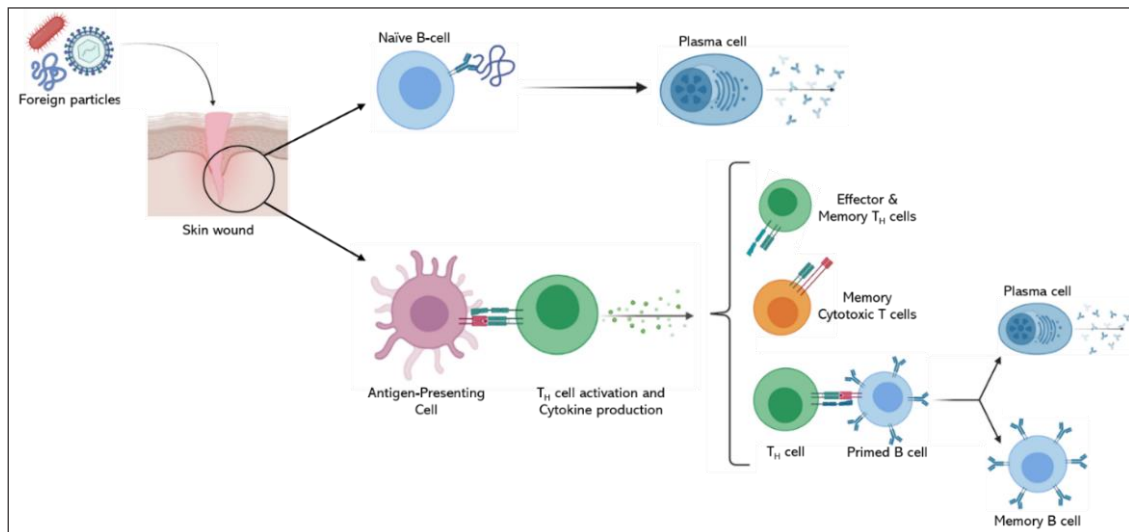
Figure 1 – Overview of the adaptive immune system. In the course of an infection by foreign particles, the APCs mediate the activation of the immune system, by presenting the antigen on the cell surface. CD4 T helper cells (T_H) are activated following the interaction of its receptors with the antigen–MHC class II complex, which leads to the release of cytokines and, therefore, the activation of cytotoxic T cells. Subsequently, activated T_H cells and cytokines lead to the differentiation and class switch of B cells into long-lived memory B cells, and into plasma cells, which secrete highly specific antibodies. Adapted from Zinsli, 2021.

B-cell response

One of the essential events of the adaptive response of the immune system is activation and differentiation of antibody-producing B cells, that occurs in germinal centres of secondary lymphoid organs. Although antibodies can act as membrane receptors of B-cells, they can also end up being secreted, binding to pathogens to either directly neutralize the pathogen, initiate the complement system or opsonize the pathogen, signalling it to be phagocytosed by other cells of the immune system [51,58].. Like TCR, antibodies are specific for the antigen, however, they additionally have the ability to recognize whole proteins, whereas the antigen presented in the context of MHC by APCs is a result of denaturation of the protein and, therefore, only a portion of it [51].

B-cells can either produce and secrete long-lived antibodies with high affinity or short-lived antibodies with lower affinity. Specifically, the humoral response can be T-cell – dependent, where B-cells are stimulated by cytokines secreted by helper T-cells, resulting in the production of high-affinity specific antibodies; or can be T-cell – independent, which is induced by the recognition of repeated patterns in foreign proteins or molecules by B cells, which leads to the production of low affinity antibodies [37,55].

The epitopes within the antigen are able to stimulate and activate T- cells (known as T-cell epitopes) or B-cells (known as B-cell epitope), and they can be either linear or conformational [55]. B cell epitopes can be identified by different methods including studying the three-dimensional structure of antigen-antibody complexes and resorting to studies where the antigen is mutated and its interaction with the antibody is assessed. The identification of T cell epitopes is usually done using MHC multimers [59].

1.4. Reverse Vaccinology and Immunoinformatics to predict novel immunogenic proteins

Immunogenicity is one of the most important properties of vaccine design and development. With the evolution of genomic sequencing techniques, the need to culture bacteria started to be replaced by techniques of reverse vaccinology and immunoinformatics, which have, thus, allowed to accelerate the search and discovery of new proteins with immunogenic potential, for application in vaccines. Vaxigen, NERVE, Jenner predict, VaxiJen and Vacceed, are analytical software programs, which were created to allow the prediction of potential vaccine candidates [60]. Although available online, they hardly have completely accessible data sets in order to identify candidate substrates broadly. Furthermore, it generally does not consider the interaction of the antigen with the cells of the immune system, focusing more on the most likely candidate, based on their conservation, their location within the cell or on the cell membrane and their adhesion properties to the host cells, among other structural and virulence characteristics.

The identification of regions or epitopes that are capable of stimulating the immune system is essential for the development of protein-based vaccines. Currently, in addition to the existence of databases for different epitopes, antigens and immunization targets, there are also *in silico* tools to predict the B-cell epitopes or T-cell epitopes.

In predicting T-cell epitopes, the goal is to identify the smallest peptides within the antigen that can stimulate both T-CD4 and T-CD8 cells. For this identification, we can follow different strategies, however, the study of the binding of peptides to MHC is the most selective technique. Both MHC class I and MHC class II have similar three-dimensional (3D) structures, however there are differences in their groove that are significant regarding peptide binding. Besides, it is also important to mention that the prediction of molecules that bind to MHC class II is less accurate than for MHC class I.

B-cell epitopes can be divided into linear epitopes – sequential residues – and conformational epitopes – portions of exposed residues, which are not necessarily sequential. In addition, antibodies that recognize linear epitopes are able to recognize denatured antigens, unlike conformational epitopes. Moreover, while linear epitopes can be predicted from the primary sequence of the antigen (using sequencing-based methods), prediction of conformational epitopes generally requires the 3D structure of the protein, which may not be available [59]. The Immune

Epitope Database (IEDB) is one of the largest databases of immunological epitopes, both for B-cells and T-cells [61]. Linked to this database there is also the IEDB – Analysis Resource (IEDB-AR), which compiles various B- and T-cell epitope prediction tools [62].

In summary, a more realistic *in silico* approach to predict novel protein immunogens from bacterial proteomes is the one that combines both reverse vaccinology and immunoinformatic tools as depicted in **Figure 2**.
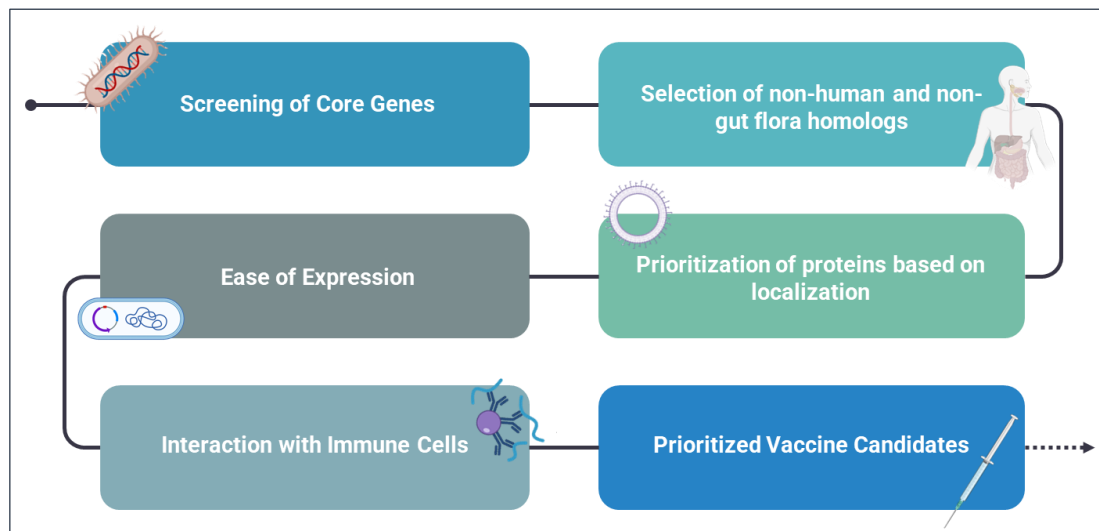
Figure 2 – Reverse Vaccinology approach. In order to select the most adequate proteins, first is important to select the core genes of the bacteria among strains, to have a broad action. Next, to prevent autoimmunity, is required to exclude human and gut-flora homologs. The following filtration of the proteins considers it localization, weight, number of helices, solubility, and other physical characteristics to facilitate their expression. Finally, is valuable to predict their interaction with the immune cells and immunogenic potential (immunoinformatics), in order to choose the best vaccine candidates.

1.5. Immunogenic Proteins as Virulence Factors

The interactions that occur between the pathogen and the human host can be studied from the perspective of the pathogen or from the host, in an attempt to identify which metabolites and/or strategies are employed during the infection [63]. Microorganisms have a large set of virulence factors in order to survive and proliferate within their hosts, leading to interaction between them and the development of infections. The virulence factors of microorganisms include secreted products or even structures present on the cell surface, such as capsules, lipopolysaccharides or glyco- and lipoproteins [64]. Understanding the biology of the pathogenic microorganism and its virulence factors is essential for the development of new therapeutic techniques.

One of the most studied interactions between the pathogens and the host is the protein-protein interactions [63]. For instance, outer membrane proteins, or porins, play a critical role in interacting and adapting to the environment, and are fundamental in virulence [65]. The outer membrane proteins of Gram-negative bacteria are found in the outer monolayer and have a variety of functions. Not only are they involved in maintaining the membrane structure and in transportation, but they also play an essential role in the process of contact between the bacteria and the host [66]. An example of this role is the outer membrane porin OmpA of *A. baumannii*, that has the ability to induce host cell apoptosis, biofilm formation, dissemination in the blood stream and interaction with epithelial cells [67]. Another example is Omp33, which is associated with resistance of *A. baumannii* to carbapenems [68]. Many of these proteins have also been identified in the literature as immunogenic proteins, and protein-based vaccines with them have already been studied, as mentioned in the subchapter 1.2. Thus, it can be proposed that virulence factors have high probability of being immunogenic targets, and vice-versa.

1.6. Aims

Immunogenic proteins have two important roles in vaccine technology against bacterial infections. In one hand, they can be used as subunit protein vaccines to immunize hosts against bacterial pathogens, using conserved protein antigen targets. On the other hand, they can be used as subunit conjugated vaccines targeting specific bacterial glycan antigens. In these vaccines, highly immunogenicity of protein carriers is linked to bacterial glycans which are, *per se*, T-cell independent antigens. Therefore, these promote a safe, robust, and T-cell-dependent long-lasting immune responses.

Given the absent of licensed vaccines against *A. baumannii*, and due the emergence in finding new treatment and prophylactic alternatives against this bacterium, is essential to characterize novel immunogenic proteins options which are the basis of subunit vaccine development. Specifically, this project aims:

1) To create a bioinformatics pipeline to predict the novel immunogenic proteins against *A. baumannii*.
2) To express and evaluate the immunogenic potential of selected proteins against *A. baumannii* in murine models.
3) To study the bacterial virulence associated with the corresponding gene products.

CHAPTER 2

Methods and Materials

2.1. Reverse Vaccinology & Immunoinformatics

Reverse Vaccinology

To screen novel immunogenic proteins for vaccine development, one needs to filter all proteins present in the bacterial proteome according to specific traits. Consequently, six main steps were followed:

1. To select conserved bacterial proteins. These are intended to achieve maximum coverage of the vaccine against a species of every genus. Such analysis was performed by both Ortholugedb 2.1. [69] and Orthovenn2 [70]. The *A. baumannii* strains compared in this analysis are listed in **Table 1, Attachment I**.

2. To avoid autoimmunity. There is always a possibility of selecting proteins that have homologs of human and gut-flora proteins. Therefore, such homologs were excluded using the Vaxign server (version 1), with the Vaxign Query program [71,72].

3. To select extracellular and outer membrane proteins. Proteins exposed on the surface of bacteria tend to be first recognised by immune cells' receptors and mediators on the blood stream and hold a role in the pathogenicity of the microorganism. Hence, the selection of bacterial external proteins either secretome/exoproteome, extracellular region, and outer membrane regions, is desired. The tool PSORTb 2.0 [73] was employed for this step.

4. To select proteins with a high adhesion probability. Since it is intended to establish a genotype-phenotype relation between immunogenic proteins and virulence factors, extracellular or outer membrane proteins have a higher likelihood of being involved in the adhesion of bacteria to the host cells. Therefore, the adhesion probability prediction from the Vaxign server (version 1) was used as a filter [71].

5. To select proteins with a higher ease of expression. Filtrations can be made based on protein topology and molecular weight. In other words, proteins should be limited to a maximum of two transmembrane helixes and have a predicted molecular weight lower than 40 kDa, to ease their purification. To do these selections, TMHMM 2.0 [75] tool was used.

6. To select proteins with a high probability of being soluble, upon expression. To facilitate the collection of the protein after its expression, it is desired that the recombinant proteins are soluble,

and not remain in the cellular debris (insoluble bodies). For this, it was used the program SOLpro[76] to predict the solubility of the proteins and use this prediction as filter in the pipeline.

Immunoinformatics

Although the previous steps allowed to select the best proteins to study in a physical and topology point of view, there is no information about the immunogenic potential of these proteins. In other words, the procedures employed above don't provide any information regarding the bound formed between the protein and the MHC or if any epitope is going to be presented to the TCRs. Also, these proteins might have a higher or lower potential of eliciting immune responses, depending on the type and number of epitopes they have. For this evaluation, several tools are available online, for the prediction of T cell and B cell epitopes. Nevertheless, we have directed our analysis to select T cell epitopes, more precisely to CD4 T-cell epitope, i.e., to identify proteins that bind to MHCII molecules.

In the present report we applied the IEDB tool: MHC class II prediction, to predict the immunogenic potential of our proteins (http://tools.iedb.org/mhcii/). The method of prediction chosen was the IEDB recommended 2.22, which uses a Consensus approach, combining NN-align, SMM-align, CombLib and Sturniolo if any corresponding predictor is available for the molecule, otherwise it uses the NetMHCIIpan method. The HLA alleles selected to predict the affinity to are listed in **Table 2, Attachment I**.

2.2. Protein's Immunogenicity Assessment

Bacterial strains, media, and plasmids

      E. coli Top10, BL21(DE3) and C43(DE3) strains were used for cloning and protein recombinant expression. Cells were grown in Luria Broth (LB) or in Luria broth agar (LBA). Vector pET28a (Addgene) was used to clone and recombinantly express proteins.

Cloning, expression, and purification of recombinant proteins

Cloning

      Genomic DNA was extracted from a single colony that was suspended in 500 µL of sterile water. Next, the sample was heated (98 °C, 15 min), centrifuged (12000 g, 5 min), and the supernatant collected.

      PCR was first performed with DreamTaq Green PCR Mastermix (Thermo Scientific) with the following primers (**Table 2**). Upon amplification, a second PCR was made with the DNA polymerase Phusion Plus (Thermo Scientific), using the following reaction: 10 µL Phusion Plus Buffer (Thermo Scientific); 2.5 µL primer forward; 2.5 µL primer reverse; 1 µL dNTPs (Thermo Scientific); 1 µL DNA; 0.5 µL Phusion Plus and 32.5 µL of sterile water. With a cycle of 98 °C for 30 s, 35 repeats of 98 °C for 10 s, 60 °C for 10 s and 72 °C for 20 s, and then at 72 °C for 5 min. Following amplification, the PCR products were cleaned using the kit DNA Clean & Concentrator (ZYMO research).

      To accelerate the cloning task, the digestion and assembly of the PCR products with the plasmid was performed by Golden Gate Assembly, recurring to a modified pET28a plasmid, dubbed pET28a-BsaI (**Figure 3**), where it was added two with Type IIS restriction BsaI sites. The primers used to amplify the gene where also designed with the same restriction sites, as shown on **Table 2**. The Golden Gate Assembly was performed using: 1 µL pET28a-BsaI (50 ng/µL); 1 µL 10x T4 DNA Ligase Buffer (Thermo Scientific); 0.5 µL T4 DNA Ligase (Thermo Scientific); 0.5 µL BsaI enzyme (Thermo Scientific); the amplified PCR products at a 1:5 plasmid:insert mass ratio, calculated with the NEBioCalculator tool (New England BioLabs); and water to reach a reaction volume of 10 µL. Next, the thermocycler was set for 25 cycles, 37 °C for 3 min and 16 °C for 4

min, followed by 5 min at 50 °C and 10 min at 80 °C [77]. The resulting product was directly transformed into *E. coli* Top10 cells and grown on LBA plates supplemented with kanamycin, at 37 °C, overnight.
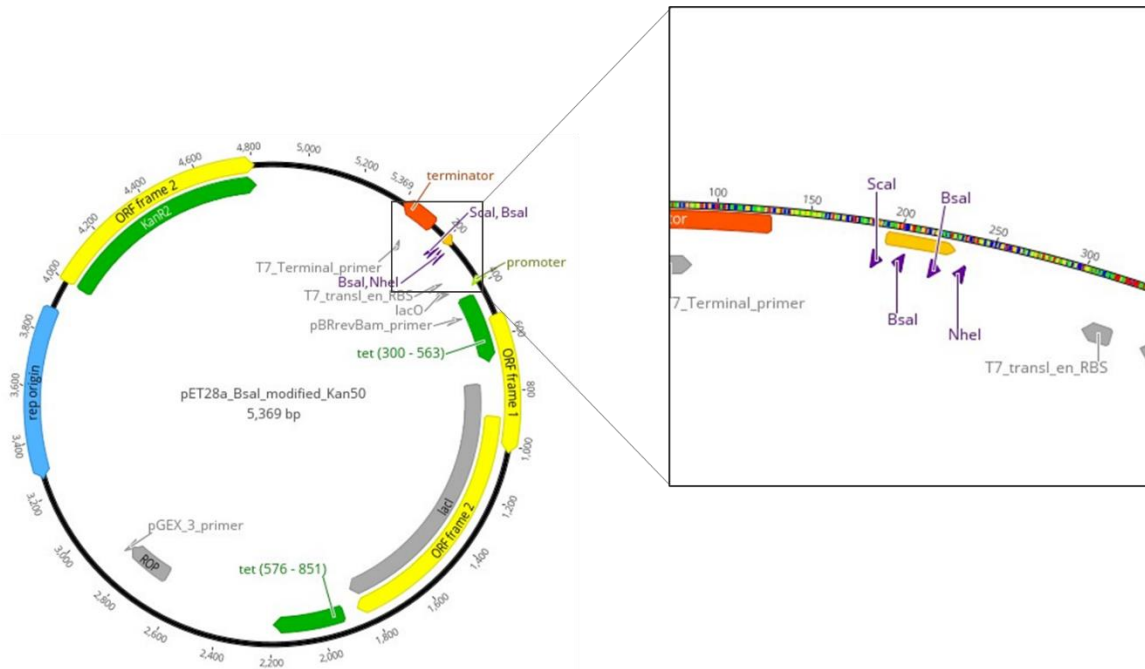
Figure 3 – pET28a-BsaI designed to perform Golden Gate Assembly.

Table 2 - Primers, enzymes, and annealing temperatures used to clone each gene. Underlined in the primers, is presented the enzyme recognition site.

Gene	Accession nº	Forward Primer	Reverse Primer	Annealing Temperature	Enzymes
BamE	WP_001170994	AAAAAA<u>GGTCTCA</u>CATG TGTTCAATCTTTGGTGT ATATAAGGTTG	TTTTTT<u>GGTCTCT</u>CTTA TAGTGGTGGGGCAGTT AAAAT	60	BsaI
Hypothetical protein (HP) 504	WP_001088069	AAAAAA<u>GGTCTCA</u>CATG TGTGCAACTACCGCAC CTCT	TTTTTT<u>GGTCTCT</u>CTTA ATCACACTTTGCTAAGT TGTCTTTAC	65	BsaI
Lipocalin	WP_000885644	AAAAAA<u>GGTCTCA</u>CATG GCATTTCGAAATAATGT TCCGCA	TTTTTT<u>GGTCTCT</u>CTTA TTCTTTATGCTCGGTAT GAATAATATCTCGA	60	BsaI

MlaD	WP_000842362	AAAAAA<u>GGTCTCA</u>CATG AAATCACGTACTAGTGA GCT	TTTTTT<u>GGTCTCT</u>CTTA CTCAACAAATGACGGC TG	60	BsaI
NlpE	WP_000749178	AAAAAA<u>GGTCTCA</u>CATG TGTAATAAACATGAAAA TAAAACAGAAACA	TTTTTT<u>GGTCTCT</u>CTTA ATCTTCTTTTTTCAAAA CATAATGTTCA	60	BsaI
Omp	WP_000698067	GGGG<u>CATATG</u>ATGAAAA TATTAAAACTATCTTTTT TAGTACTCG	GGGG<u>CTCGAG</u>TTAGAA ATGTGCTTCTAAGCC	60	NdeI & XhoI
Omp33	WP_000733005	AAAAAA<u>GGTCTCA</u>CATG TATCAATTTGAAGTTCA AGGTCAAT	TTTTTT<u>GGTCTCT</u>CTTA GAAACGGAATTTAGCAT TTAAGCC	60	BsaI
OmpA	WP_000777882	AAAAAA<u>GGTCTCA</u>CATG GGCGTAACAGTTACTC CATTAC	TTTTTT<u>GGTCTCT</u>CTTA TTGAGCTGCTGCAGGA GC	60	BsaI
OmpA2	WP_001202415	AAAAAA<u>GGTCTCA</u>CATG TGTCAAACAACAGGTAA TAACCT	TTTTTT<u>GGTCTCT</u>CTTA TTGTTTAGCGTAAATGC TGATT	60	BsaI
OmpW	WP_000475288	GGGG<u>CATATG</u>GTGTTC AAAAAAGTATTAGTTGT TGC	GGGG<u>CTCGAG</u>TTAGAA TTTATAGCTATAACCTA AAGTGTAAACAA	60	NdeI & XhoI
Putative porin	WP_000731728	AAAAAA<u>GGTCTCA</u>CATG AAAAAACTAGCAATTGC ATCAGCT	TTTTTT<u>GGTCTCT</u>CTTA GAAGCGGTATGCTGCA C	60	BsaI

Electrocompetent cells

For transformation, electrocompetent (EC) *E. coli* Top10, BL21(DE3) and C43(DE3) cells were prepared. Succinctly, a single bacterial colony of *E. coli* was grown in 5 mL of LB medium supplemented with kanamycin (LB-km) at 37 °C at 120 rpm overnight. The bacterial culture was diluted (1:100) in 100 mL of fresh LB-km medium in the following day and incubated to an optical density (OD) at 600 nm of 0.3. Cells were pelleted (4000 xg, 5 min, 4 °C), and resuspended in 40 mL, 20 mL, and 10 mL of ice-cold 10% glycerol (Thermo Scientific). Lastly, the cells were resuspended in 500 µL of ice-cold 10% glycerol, distributed by aliquots of 80 µL and kept at -80 °C.

Electroporation

For transformation, 80 μL of EC cells were transformed with 1 ng of plasmids with 1.8 KVolts. Next, cells were incubated with super optimal broth (SOC) medium, at 37 °C for 1 hour, and finally plated in agar plates with the proper antibiotic.

Colony PCR

After transformation, colony PCR was performed using the following reaction: 3 μL Xpert Taq Mastermix 2x (Grisp); 0.5 μL primer T7 forward; 0.5 μL primer T7 reverse; 1 μL sterile water and 1 μL of DNA. With a cycle of 95 °C for 5 min, 35 repeats of 95 °C for 20 s, 49 °C for 20 s and 72 °C for 45 s, and then 5 min at 72 °C. PCR products were separated under 1% agarose gels and visualized with the ChemiDoc. Positive transformants were grown in fresh agar plates supplemented with proper antibiotic.Then, recombinant plasmids were extracted with the kit NucleoSpin® Plasmid (Machery-Nagel) and sent to Sanger Sequencing for confirmation (Eurofins).

Protein Expression

A small-scale expression was first performed to assess if the protein was soluble or insoluble. For this, 5 mL of *E. coli* BL21 cells harbouring the plasmids were grown until reaching an $OD_{600\ nm}$ of 0.5-0.6 and the protein expression was induced with 1 mM of β-D-1-thiogalactopyranoside (IPTG, Thermo Scientific) for 16 h at 16 °C with an agitation of 160 rpm. Next, cells were centrifuged (9,500 xg, 5 min, 4 °C), suspended in 1/10 volumes of lysis buffer (20 mM NaH_2PO_4, 0.5 M NaCl, pH 7.4), disrupted by three cycles of freeze-thawing (-80 °C to room temperature) and sonicated (Cole-Parmer, Ultrasonic Processors) for 5 cycles (30 s pulse, 30 s pause). Insoluble cell debris was removed by centrifugation (9,500 xg, 15 min, 4 °C), the supernatant was collected, and the insoluble fraction was suspended in the same volume of lysis buffer as before. Fractions (100 μL) collected at different time points were visualized in sodium dodecyl sulphate polyacrylamide gel electrophoresis (SDS-PAGE) gels under denaturation conditions. To perform the electrophoresis, a 4% upper stacking and a 12% lower separating acrylamide gels were prepared. From the samples gathered, 15 μL were added to 4 μL of SDS-PAGE sample loading buffer (5x, NZYTech), boiled at 95 °C for 5 min and loaded onto the gels together with the protein ladder. Protein bands were routinely separated for approximately 90 min

at 120 volts. Next, gels were stained with BlueSafe (NZYTech). To express the proteins at a higher scale, it was followed the same protocol as above, however in a 100 mL volume of bacterial culture.

Protein purification

Depending on the solubility of the recombinant proteins heterologous expressed, different protocols were applied.

For soluble proteins, the insoluble cell debris was removed by centrifugation (9,500 xg, 15 min, 4 °C) and the supernatant was collected, filtered (0.22 μm filters, Whatman TM) and applied to affinity gravity chromatography columns containing Ni^{2+}-NTA resins (Thermo Scientific) for purification, using protein-dependent imidazole concentrations (25 – 250 mM imidazole). The eluted protein fractions were visualized by SDS-PAGE gels, following the same procedure as aforementioned.

For insoluble proteins, the insoluble cell debris was suspended twice in 5 mL of lysis buffer 0.5% in Triton X-100, agitated at 120 rpm, room temperature (RT), for 10 min, and centrifuged (9,500 xg, 5 min, 4 °C) and then in 5 mL of lysis buffer and centrifuged. The insoluble cell debris was solubilized in 3 mL of PBS buffer, 8 M in urea, and incubated overnight, at RT, and at 120 rpm. Next, the sample was centrifuged (9,500 xg, 10 min, 4 °C), the supernatant collected, dialysed, and purified by affinity chromatography.

If expression was not observed, plasmids were transformed and expressed in EC C43 cells, which are designed for membrane and toxic proteins expression [78], using equal protocols.

Structural analysis

Circular Dichroism (CD) was performed to ensure the proper folding of the proteins. CD experiments in the far- and near-UV region were performed using a Jasco J-1500 CD spectrometer. The spectra were recorded in a cell width of 0.1-mm path length from 190 to 250 nm for all proteins with 1 nm steps, scan speed of 20 nm/min, high sensitivity, and a 16 s response time. The samples were analysed with an average concentration of 0.15 μg/μL. Two consecutive scans for each sample and its respective buffer baseline were obtained. The averaged baseline spectrum was subtracted from the averaged sample spectrum measured under the same conditions.

Secondary structure estimates were derived from the spectra and compared to the secondary structure, predicted using PSIPRED server [79].

Immunogenicity assessment

Ethical Issues

Animal experimentation was performed in the Life and Health Sciences Research Institute (ICVS) of University of Minho. ICVS holds a license in accordance with European guidelines for the care and use of animals for research purposes (**Attachment II**). Experiments were performed under the supervision of my co-supervisor Alexandra Fraga, who has Category C – FELASA certification to perform animal experimentations (FELASA).

Endotoxin Quantification

Before inoculating recombinant protein in mice, the level of endotoxins present was quantified, using the kit Pierce™ Chromogenic Endotoxin Quant Kit (Thermo Scientific), and following the manufacturer's instructions.

The quantification of LPS in the samples to be immunized was done for a protein concentration of 0.20 µg/µL, since this was the concentration implemented for the immunization. As indicated by the producer, a calibration curve was performed (**Figure 1, Attachment III**), from which was extrapolated the **Equation 1**, used to quantify the amount of endotoxin units (EU) per mL present in the samples.

$$OD_{405nm} = 1.006 \times [EU] - 0.057 \quad (\textbf{\textit{Equation 1}})$$

Mouse Immunization

Recombinant proteins (Omp33, NlpE and BamE) were added to aluminium hydroxide adjuvant (Imject® Alum, Thermo Scientific) in concentration of 0.2 µg/µL and in a proportion of 1:1, according to manufacturer instructions. Groups of mice (n = 8), 3 males and 5 females, were immunized intraperitoneally with 200 µL of the prepared solution. The groups were immunized at 3 time points (days 0, 15 and 30), and blood samples were collected at 4 different time points (days -1, 14, 29 and 45), as schematized in **Figure 4**. Next, mice were sacrificed through

asphyxiation with carbon dioxide, to collect the blood and to harvest the organs to perform histology assays.

As negative controls we used a group of 5 mice immunized with PBS buffer combined with aluminium hydroxide adjuvant vehicle, in a proportion of 1:1.
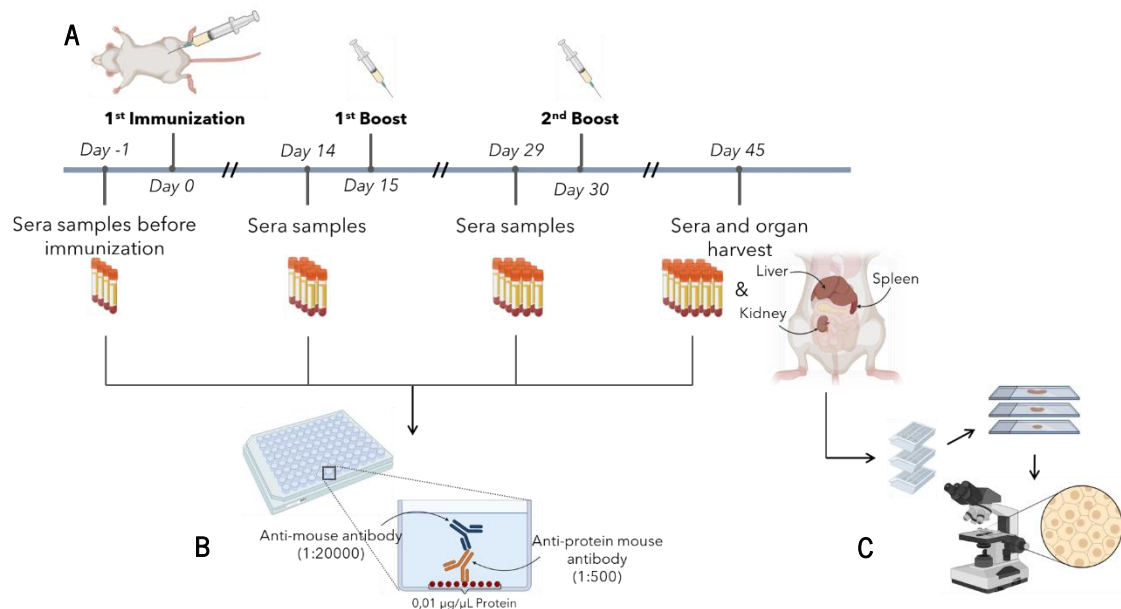
Figure 4 – Plan of the immunization of mice (A) and further ELISA (B) and histology (C) assays. The mice were immunized at days 0, 15 and 30, and blood samples were collected before immunization and at days 14, 29 and 45. on the 45th day, mice were sacrificed, and the liver, and spleen were harvested to be further evaluated by histology. For this, the organs were fixed in 3.7% formaldehyde for a week, under agitation, and later sectioned and stained with HE to be microscopically assessed. The sera samples collected throughout the research were all analysed by ELISA assays.

ELISA Assays

   ELISA assays were performed using 96 wells plates (Thermo Scientific) coated with 0.01 µg/µL of each one of the tested proteins and incubated overnight at 4 °C. Bovine serum albumin (BSA) was used as a negative control. The next day the plates were washed five times with 200 µL of PBS 1x buffer, blocked with 200 µL PBS 1x, 1% (w/v) in BSA, and incubated at room temperature for 1 h, under agitation. Next, the plates were washed five times with PBS 1x, 0.05% (v/v) in Tween 20, and added 100 µL of mice serum collected, diluted in PBS 1x buffer in a proportion of 1:500, and incubated for 2 h at 37 °C. Later, the plates were washed as previously, added 100 µL of diluted Pierce goat anti-mouse IgG, (H+L), horseradish peroxidase conjugated, detection antibody (Thermo Scientific) with a dilution of 1:20000, and incubated at room temperature for 1 h, in the dark. After, the plates were washed, added 50 µL of 3,3,5,5-Tetramethylbenzidine (Thermo Scientific) and incubated for 15 to 30 min, to reveal the secondary antibody. Finally, it was added 50 µL of 2M sulfuric acid solution to stop the reaction and measured the absorbance at 450 nm. The distribution of the serum in the ELISA plates is shown in **Figure 5**. The statistical significance between the values obtained from each timepoint, and between control and tested group was determined by a Two-Way ANOVA and Tukey's multiple comparisons test with a 95% confidence interval.
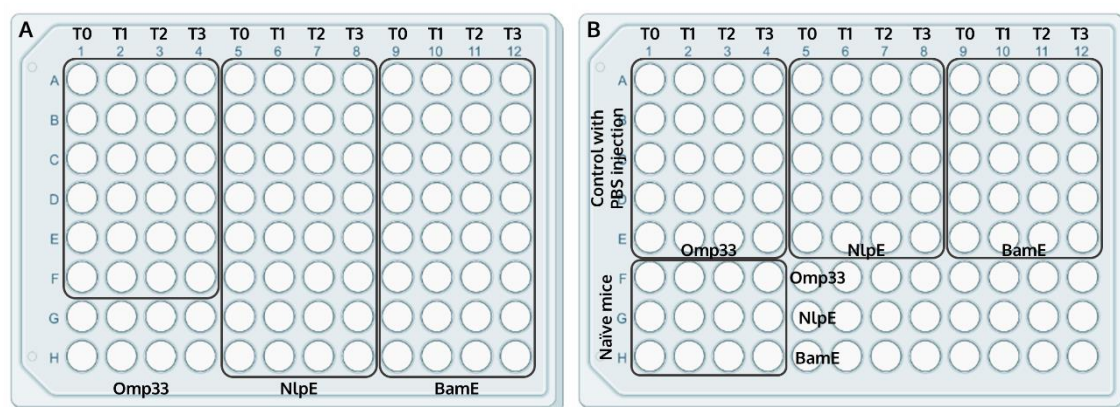
Figure 5 – Schematization of serum's distribution for ELISA assays. Plate A shows the distribution of the injected mice's serum with each of the proteins. The lines correlate to the mice and the columns correspond to each time point of the blood sample. Plate B shows the distribution of the serums from the control mice. The control mice's serum was evaluated for each protein, at the different time points. Here the lines correspond to each of the proteins, and the columns represent the mice from which the blood was collected. T0 – Timepoint zero; T1 – Timepoint 1; T2 – Timepoint 2, and T3 – Timepoint 3.

Histology Assays

Upon animal sacrifice, the liver and spleen were harvested and incubated in buffered formaldehyde 3.7% for, approximately, one week, at room temperature and under agitation, followed by paraffin embedment. Formalin-fixed paraffin-embedded tissue specimens were then sectioned and stained with Hematoxylin-Eosin for microscopic evaluation.

2.3. Virulence evaluation

Bacterial strains, media, and plasmids

A. baumannii strain ATCC 19606 was grown at 37 °C in trypticase soy broth (TSB) or in trypticase soy agar (TSA). Additionally, plasmids pCasAb-apr (Addgene) and pSGAb-km (Addgene) were used to genome editing of bacterial cells.

Genome Editing

Electrocompetent cells

For the CRISPR/Cas9 genome editing approach, it was necessary to prepare EC wild-type (WT) *A. baumannii* cells and EC *A. baumannii* cells harbouring the pCasAb plasmid. For this, a single bacterial colony of *A. baumannii* was grown in 5 mL of TSB medium at 37 °C and 120 rpm overnight.

The overnight culture was diluted (1:100) in 50 mL of fresh TSB medium in the following day and incubated to an OD at 600 nm of 0.5 (for WT cells) or just 0.15 (for cells harbouring pCasAb and in presence of 50 µg/mL apramycin). Cells were pelleted (4,000 xg, 5 min, 4 °C), and resuspended in 15 mL of ice-cold sterile water and 15 mL of ice-cold 10% glycerol (Thermo Scientific). Cells were then resuspended in 500 µL of ice-cold 10% glycerol, distributed by aliquots of 80 µL and kept at -80 °C. In case of cells harbouring the pCasAb plasmid, an additionally step was done, by adding 50 µL of IPTG to the culture, once it reached the desired OD, and incubated 2h at the same growth conditions, to express the Cas9 enzyme and the recombinases.

Electroporation

For transformation 80 µL of EC cells were transformed with 50 ng of plasmids with 2.5 KVolts and grown with SOC medium, at 37 °C for 1 hour, and finally plated in agar plates with the proper antibiotics. Plates grew overnight at 37 °C. Of note, only fresh induced EC cells harbouring pCasAb were used for genome editing.

Spacer Cloning

To jumpstart the genomic edition first the spacers (**Table 3**) were constructed and cloned into a sgRNA plasmid, pSGAb-km. Therefore, 1 μL of the 20 bp spacers (100 μM) were phosphorylated at 37 °C for 1h, with 1 μL of T4 Polynucleotide Kinase (Thermo Scientific), 5 μL of 10x T4 DNA Ligase Buffer (Thermo Scientific) and 42 μL of sterile water. Following the phosphorylation, it was added 0.5 μL of 5M NaCl to the spacers, incubated at 95 °C for 5 min and cooled down to RT, 1 °C per 10 s. Next these were cloned into the plasmid pSGAb, by Golden Gate Assembly, using the same reaction as mentioned above. Then, 1.5 μL of the assembled product was transformed into 80 μL EC Top10 cells and grown overnight in LB agar plates with kanamycin, at 37 °C.

Table 3 – Spacers and Donor DNA designed for knockout of the genes.

	Spacer Forward	Spacer Reverse	Donor DNA
Omp33	TAGTCCTAACTTCTTAA TGACTGT	AAACACAGTCATTAAG AAGTTAGG	CCTTACCTTCCTGTATATGCTAGCGCAACTTACAACCACACT GCTGCTATCCAAAACGACCAAGATGCTGTTACAGCACG
BamE	TAGTATCCCCTCAATC CACAACGT	AAACACGTTGTGGATT GAGGGGAT	TCCTCAAGGGACTCCATTGACTAAAGCTCAAGCCTCTCAAAT GGTCAGCATTTAAAAATTTACTTTGATGGAACTGGAAC
NlpE	TAGTGAGCTAACAGAA ACCTATCT	AAACAGATAGGTTTCT GTTAGCTC	CTACTCCTGTACAAACTGCTCAATCAAATAATAATGAAGCGGT AAAGGTGATGCAAACCCATTTGAAACCCATGGTAAGT

After transformation, colony PCR was performed following the procedure above mentioned, using the spacer forward and the M13 reverse primer. Positive transformants were grown in fresh LB plates supplemented with kanamycin and their plasmids extracted with the NucleoSpin Plasmid kit and sent to Sanger Sequencing for confirmation.

Two-plasmid-system genome editing

Upon the confirmation with Sanger Sequencing, 200 ng of pSGAb plasmid cloned with the spacers were transformed into 80 μL of EC *A. baumannii* cells, with the Cas9 and recombinases induced. 3 μL of the donor DNA (**Table 3**) was transformed together with the plasmid, incubated at 37 °C for 1 hour, plated in TSA agar plates supplemented with apramycin and kanamycin and allowed to grow overnight at 37 °C. Alongside, it was also transformed 200 ng of the pSGAb plasmid

and 200 ng of pSGAb cloned with spacers into EC pCasAb-harbouring *A. baumannii*, incubated at 37 °C for 1h, plated in TSA agar plates with apramycin and kanamycin and grown overnight at 37 °C, to act as positive and negative controls, respectively.

Colony PCR was performed as aforesaid, with the primers shown on **Table 2**, together with the forward spacer (**Table 3**), according on the gene deleted. PCR products were separated under 3% agarose gels and visualize with the ChemiDoc. Positive colonies were grown in fresh TSA plates supplemented with kanamycin and apramycin. The muted gene was then amplified trough PCR with DreamTaq MasterMix, cleaned with the kit DNA Clean & Concentrator, and sent to Sanger Sequencing for confirmation, with the specific primers from **Table 2**.

Plasmid curing

To cure the pSGAb and the pCasAb plasmids, the confirmed *A. baumannii* mutant was grown in 5 mL of TSB (overnight at 37 °C and 120 rpm). The next day a fraction of the culture was plated into TSA agar plates supplemented with 5% w/v sucrose and grown overnight at 37 °C. Several colonies were then plated onto TSA agar plates with each of the antibiotics, and TSA agar plates without any antibiotics, and grown overnight at 37 °C. When the colonies grew only in the plates without any antibiotic, the plasmids were cured, and the mutant cryopreserved.

Virulence Assays

Growth Assays

A culture of each mutant strains and of the WT strain were grown overnight, diluted 100x in 10mL of TSB and grown at 37 °C and at 120 rpm. Their growth was monitored within time points of one hour between each, for a period of 7 h. Three repeated experiments were performed, and the data distribution analysed to exclude outliers. Thus, averages and standard deviations are given, as well as the growth kinetics rate and the duplication time for each mutant, obtained by the linearization of the exponential growth phase.

In the linearization of the exponential phase, the slope of the equation resulting, corresponds to the exponential growth rate, from which it is calculated the value of the duplication time, using **Equation 1**, **Attachment IV**. The linearization of the curves is shown on **Figure 1**, **Attachment IV**. The equations obtained for the WT strain and for each mutant *Δomp33*, *ΔnlpE* and

ΔbamE (Equations 2 – 5, **Attachment IV**), were extrapolated from the linearization following the structure of **Equation 2**.

$$LN\ (Strain) = Slope \times Incubation - LN(Incubation = 0)\quad (\textbf{Equation 2})$$

Biofilm Assays

Biofilms were formed on 96-well polystyrene microtiter plates using established protocols with minor modifications [80]. *Acinetobacter* cultures were first grown for 16 h at 37 °C and 120 rpm and then diluted 1:100 in TSB. Each well was inoculated with 200 µL of this bacterial suspension and the microtiter plates were incubated for 24 h and for 48 h at 37 °C and 120 rpm. Next, the wells were washed with saline solution (NaCl 0.9%) two times, the biofilm fixed by adding methanol 100%, and the adhered cells were quantified by staining with crystal violet 1% (v/v) at 570 nm and solubilization with acetic acid 33%. In the 48 h assays, the medium on the microplates was changed after 24 h of incubation, and the same procedure was followed. The statistical significance between the data obtained from each mutant and WT was determined by an Unpaired t-test, and between time of growth was determined by multiple t-tests (95% confidence interval). Additionally, the outliers were excluded, and is shown the optical density values obtained, alongside the standard deviations.

Human Serum Assays

Overnight cultures of the *A. baumannii* cells (WT and Δomp33, ΔnlpE, ΔbamE mutants) were diluted in TSB to 10^4 CFU/mL and were added to human serum collected from healthy volunteers at a 1:3 volume ratio. Next, infected serum was incubated for 1 h at 37 °C. Similar samples supplemented with decomplemented serum (at 56 °C for 30 min) were used as positive controls. Survival bacterial cells were determined by colony forming units (CFUs) counts. Significance between values was determined by Multiple t-test and between mutants by Two-Way ANOVA (95% confidence interval). Averages and standard deviations of three repeated experiments are given.

CHAPTER 3

Data Analysis and Discussion

3.1. Reverse Vaccinology and Immunoinformatics

Through reverse vaccinology, comparative analysis of 10 *A. baumannii* strains at OrtholugeDB, revealed 2542 core genes were obtained. After exclusion of human and gut-flora homologs, 1389 genes remained, of which only 61 were extracellular or were located in the outer membrane. Coincidentally, none of these proteins had more than 2 helices and, therefore, those with molecular weight lower than 40,000 g/mol were selected. At the end, 21 protein-encoding genes remained (**Table 3**, **Attachment I**), for which their immunogenic potential was predicted (**Table 4**, **Attachment I**). The majority of proteins identified by our pipeline were also found in previous studies made using reverse vaccinology [81] or proteomic approaches [82].

Immunoinformatics, otherwise known as computational immunology, can further be used to selected proteins with higher immunogenic potential. These tools can be used to screen protein sequences and identify regions with a higher affinity of binding to MHC molecules and be presented to the adaptive immune system. The MHC class II complexes are heterodimeric glycoproteins which, in humans, are encoded in the human leukocyte antigen (HLA) gene complex, with several allelic variants, which means that there is a massive diversity of MHC structures. Furthermore, most MHCII molecules are represented with very little binding information, limiting the available affinity prediction methods. Additionally, even though the binding affinity between the peptide and MHCII is essentially determined by the peptide core sequence, peripheral amino acids affect binding to the molecule [83]. All these factors complicate the prediction of the binding affinity of peptides to MHCII, affecting its efficiency.

Despite the limiting accuracy of prediction tools for MHCII complexes, these were chosen since it is intended to induce a humoral response and the production of memory cells. As mentioned in chapter III, MHCII present antigens that are recognized by CD4 T cells, which then engage in the release of cytokines and triggering the development of effector T cells, B cells, high specific antibodies, and memory B cells. By its turn, MHCI activate CD8 T cells, which have a killing function and do not lead to the production of memory B cells nor the production of antibodies. Thus, the identification of CD8 T cell epitopes would be obsolete to this work.

In the IEDB: MHC class II prediction tool it is requested the sequences to be analysed, the prediction method and the human alleles to specify the binding predictions. For the sequence, the 21 proteins selected were imported, the prediction method used was the recommended one (IEDB

recommended 2.22) and the alleles selected belonged to the HLA-DRB1 gene. Additionally, according to the Allele Frequency Net Database (http://www.allelefrequencies.net/default.asp), these alleles are very frequent in the Portuguese population, allowing us to direct the potential vaccines to this population. Nevertheless, no conclusive results were obtained in the 21 proteins earlier selected, when evaluated through this tool, possibly due to the stated limiting efficiency. However, despite this output, we noticed that some of the 21 candidates selected by reverse vaccinology were described in the literature as licensed immunogenic proteins, reinforcing the robustness of our pipeline to selected candidates for vaccine development. Additionally, some of these proteins were also pointed as having virulence roles [39,40,46,84–86]. Even though the results were obtained go accordingly to ones previously publish, an additional step was added to assist the selection of proteins in further phases: the prediction of the protein's solubility, using the SOLpro tool. The resulting protein candidates for *A. baumannii* subunit vaccines are shown on **table 5**, alongside the solubility prediction. Overall, using this approach and given the fact that a typical *A. baumannii* has approximately 3500 coding sequences, only 1% are predicted to be of potential use in vaccine development. Furthermore, only 38% of the potential vaccine candidates were predicted to be soluble, which could explain the difficulty in the development of such vaccines.

Table 4 – *A. baumannii* immunogenic proteins candidates. Proteins selected by reverse vaccinology tools, as *A. baumannii*'s immunogenic proteins, alongside their position in the cell, solubility prediction by SOLpro and if they are pointed as immunogenic in literature.

	Protein	Location	Immunogenic	Solubility prediction
A. baumannii ATCC 17978	Outer membrane beta-barrel protein, OmpW homolog	Outer Membrane	No	Soluble
	Hypothetical protein 67	Extracellular	No	Insoluble
	OmpA family protein (OmpA2)	Outer Membrane	No	Soluble
	Outer membrane protein assembly factor BamE	Outer Membrane	No	Soluble
	Copper resistance protein NlpE	Outer Membrane	No	Soluble
	Tetratricopeptide repeat protein 3	Extracellular	No	Soluble
	Hypothetical protein 322	Outer Membrane	No	Soluble
	Porin	Outer Membrane	No	Insoluble
	Type VI secretion system tube protein Hcp	Extracellular	Yes [85]	Soluble
	Peptidoglycan DD-metalloendopeptidase family protein 2	Outer Membrane	No	Insoluble
	Pal	Outer Membrane	No	Insoluble

Plug domain-containing protein	Extracellular	No	Insoluble
OmpA-1 family protein	Outer Membrane	Yes [41]	Insoluble
Outer membrane lipid asymmetry maintenance protein MlaD	Extracellular	No	Insoluble
Hypothetical protein 504	Extracellular	No	Soluble
GspH/FimT family pseudopilin 2	Extracellular	No	Insoluble
Pilin	Extracellular	No	Insoluble
Porin Omp33-36	Outer Membrane	Yes [45]	Insoluble
Putative protein, pporin homolog	Outer Membrane	No	Insoluble
M23 family metallopeptidase	Outer Membrane	No	Insoluble
TiGR04219 family outer membrane beta-barrel protein, omp homolog	Outer Membrane	No	Insoluble

3.2. Protein's Immunogenic Evaluation
Protein Cloning, Expression and Purification

To clone genes, we used a previously modified version of pET28a available in-house (pET28a-BsaI). Based on predicted solubility and molecular weight, 11 genes were selected to be cloned with and without signal peptide coding sequences: *omp33, ompA, omp, ompW, lipocalin, pporin, nlpE, ompA2, mlaD, bamE* and *hp504*. The agarose gels from the colony PCRs performed showing the positive colonies obtained are shown on **Figure 6**.
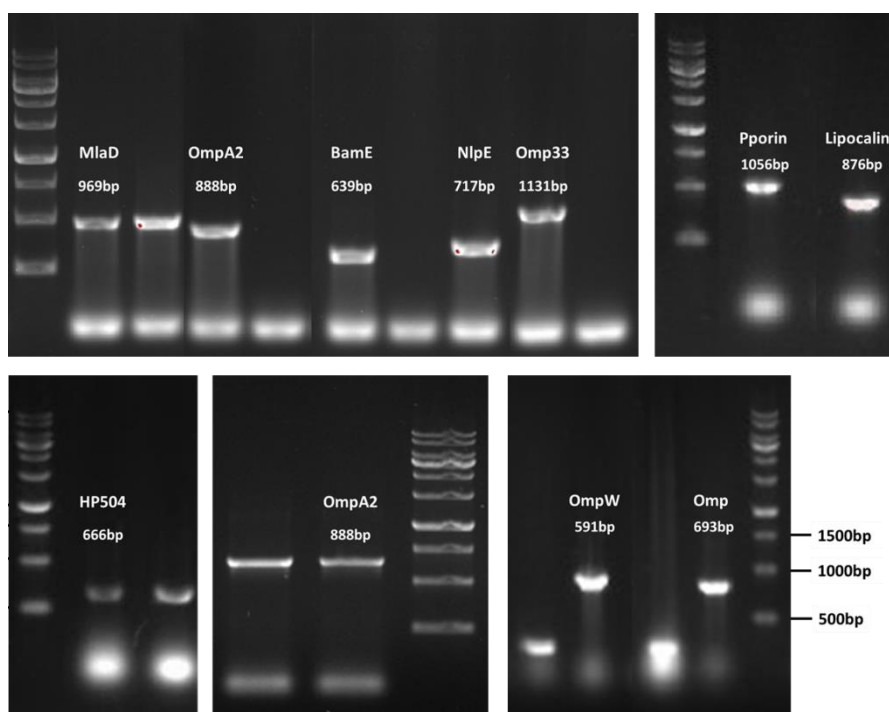
Figure 6 – Agarose gels from the positive colonies with the cloned genes. The genes shown were amplified and cloned into the pET28a-BsaI plasmid and grown in EC *E. coli* Top10 cells. Here are shown positive colonies obtained for each cloned gene.

Results showed that BL21 did not induce recombinant expression, even after several attempts and changing the expression conditions (**Figure 1**, **Attachment V**). Even when expressed with C43 cells, protein synthesis was not obtained (**Figure 2**, **Attachment V**). Given the fact that signal peptides might influence the heterologous expression, we decided to, initially, re-clone and express *omp33* without the signal peptide. After the induction of expression, we saw that the absence of this sequence enhanced the expression of the recombinant protein, as seen in **Figure 7**.

Figure 7 – **Difference between expression of protein Omp33 with and without signal peptide.** The resulting SDS-PAGE gels show that the protein Omp33 is barely expressed by *E. coli* BL21 with the signal peptide. But when this region was removed, expression increased substantially. The ladder used was PageRuler Unstained Broad Range Protein Ladder (Thermo Scientific). NI – not induced; I – induced; SF – soluble fraction; IF – insoluble fraction.

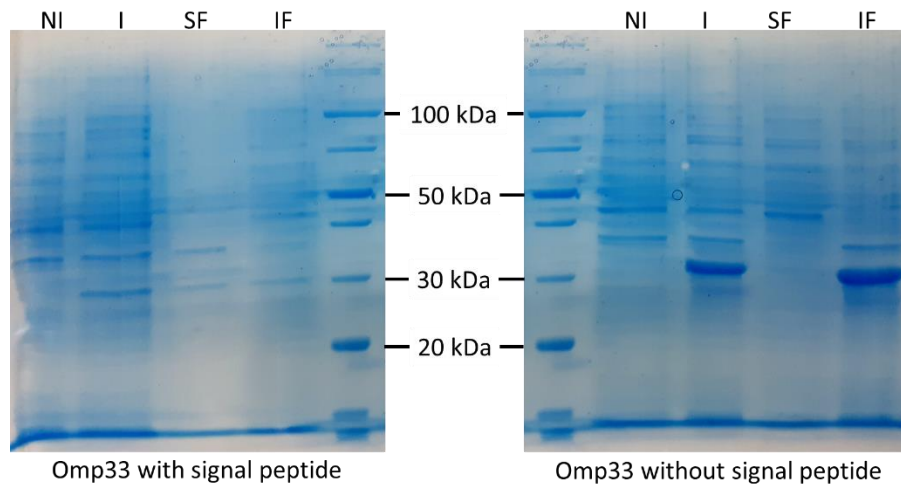According to literature, the deletion of a transmembrane or hydrophobic patch region of the signal peptide, frequently leads to an increased expression of the gene and of the solubility of the protein [87]. Since the signal peptide is not present in the mature protein and does not alter its biochemical properties or function. Thus, the remaining genes (*ompA, nlpE, ompA2, mlaD, bamE, hp504*) were re-cloned and expressed without their signal peptides. After small scale expression, all proteins were successfully expressed (**Figure 3**, **Attachment V**), however only the proteins NlpE and BamE were soluble. Comparing the results obtained with the prediction from SOLpro, it was noted that this tool had an accuracy of approximately 71%, meaning that it could be employed in future studies. Thus, NlpE and BamE were chosen to further be expressed at a higher scale and for the *in vivo* assays. Additionally, given that the Omp33 protein is an immunogen [45], it was also chosen to act as a baseline value for the results obtained. Hence, proteins NlpE, BamE and Omp33 were expressed in a 100 mL *E. coli* BL21 culture, yielding concentrations of 3.55 µg/µL, 5.33 µg/µL, and 0.721 µg/µL, respectively. The obtained the SDS-PAGE gel for these proteins can be seen in **Figure 8**.

As Omp33 is insoluble, it was necessary to recover the protein from the inclusion bodies. Therefore, the protein was denaturated using urea, renaturated through dialysis and purified by affinity chromatography.
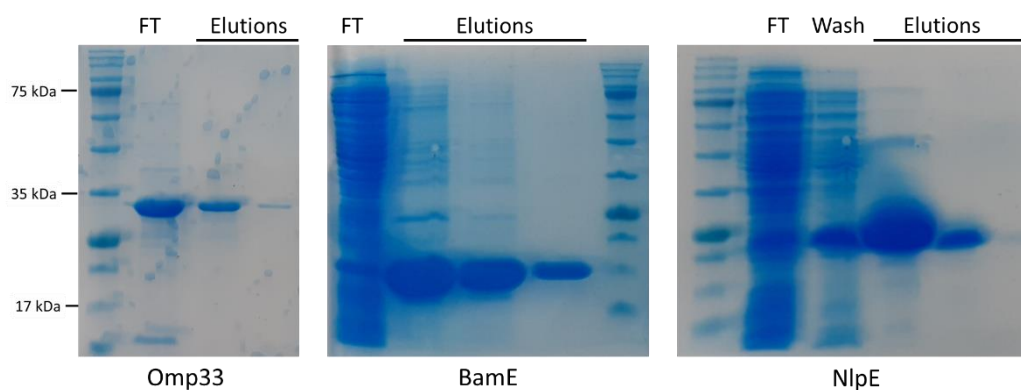
Figure 8 – Omp33, BamE and NlpE SDS-PAGE gels. The gels show that the soluble proteins – NlpE and BamE, were highly expressed. The Omp33 protein's gel show that protein obtained after dialysis and purification through affinity chromatography. The ladder NZYColour Protein Marker II (NZYTech) was used in all gels. FT – flow trough.

Structural Analysis

To confirm the proper refolding of the Omp33 protein, the protein was evaluated by Circular Dichroism (CD), alongside the proteins NlpE and BamE. The circular dichroism provides information about the protein's secondary structure, derived by the absorption of left- and right-circularly polarized light [88]. The results obtained are present in **Figure 9**, alongside the prediction of their secondary structure projected by the server PSIPRED.

Figure 9 shows CD spectra of the proteins. Omp33 has a maximum peak at around 195 nm and a minimum peak at around 215 nm, suggesting that it folds predominantly by β-sheets. BamE show a maximum peak at around 192 nm and two minimum peaks at around 220 nm and 208 nm, associated with proteins rich in α-helix secondary structures. Lastly, for NlpE, a minimum peak at around 195 nm suggests a random coil. Moreover, CD secondary structure prediction agrees with PSIPRED program. Therefore, all proteins, expecting are properly folded, including Omp33 that had to be renatured.
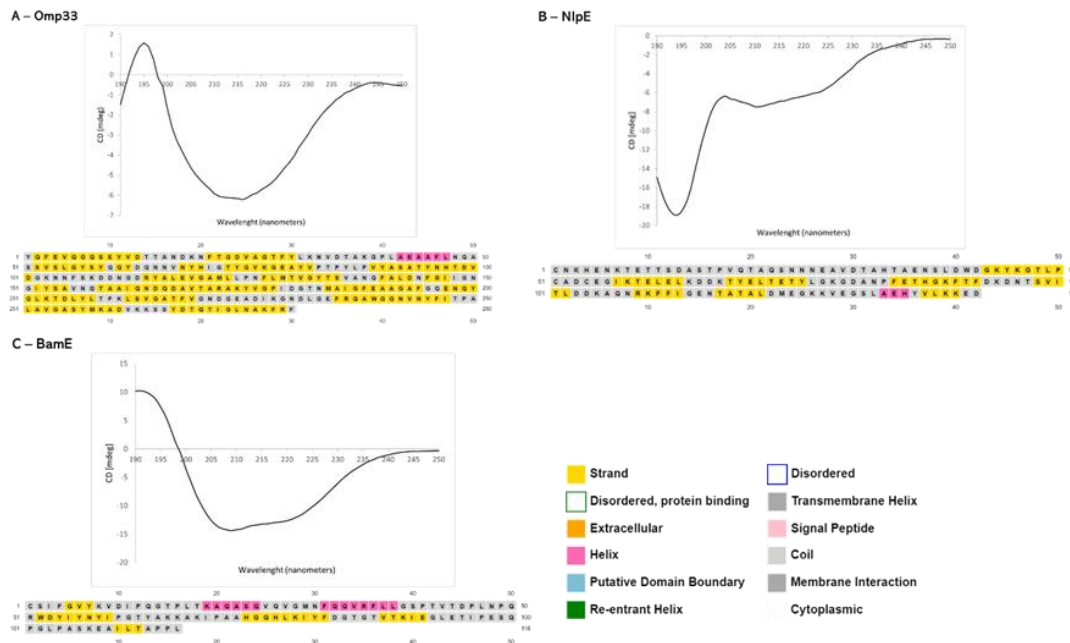
Figure 9 – Spectra obtained by the CD analysis. This analysis was performed for the proteins Omp33 (A), NlpE (B) and BamE (C). Alongside, there are shown charts of the structure prediction by PSIPRED program. An α-helix structure is shown by a maximum peak at 192 nm and by two minimum peaks at 208 and 220 nm; a β-sheet structure is shown by a maximum peak at 195 nm and a minimum peak at 215 nm; and a random coil is represented by a minimum peak at 195 nm.

Endotoxin Quantification

Sepsis refers to systemic inflammatory response syndrome caused by exacerbated infection, due the presence of infection factors, such as LPS. These activate the inflammatory response, resulting in the production and release of multiple inflammatory mediators [89]. It can lead to the death of patients and animal models in scientific studies. Since the recombinant proteins were synthesized in *E. coli* and being this a Gram-negative bacterium, in the recovery and purification of the proteins there may be traces of LPS in solution. Hence the need to quantify the amount of LPS present in the samples.

As mentioned, **Equation 5** was used to quantify the concentration of endotoxins present in the samples. The values of endotoxins obtained for the proteins Omp33, NlpE and BamE were 1.157 EU/mL, 1.185 EU/mL, and 1.125 EU/mL, respectively. These values were considered acceptable for the immunization of mice, without risking septic shock, given that in former studies involving immunization of mice, samples with residual endotoxin concentrations below 30 EU/mL

and around 1 EU/mL were administered in mice, without any septic response reported [38,39,41].

Immunogenicity Assessment

ELISA assays were performed according to the scheme in **Figure 5**, and the results are shown in **Figure 10.**
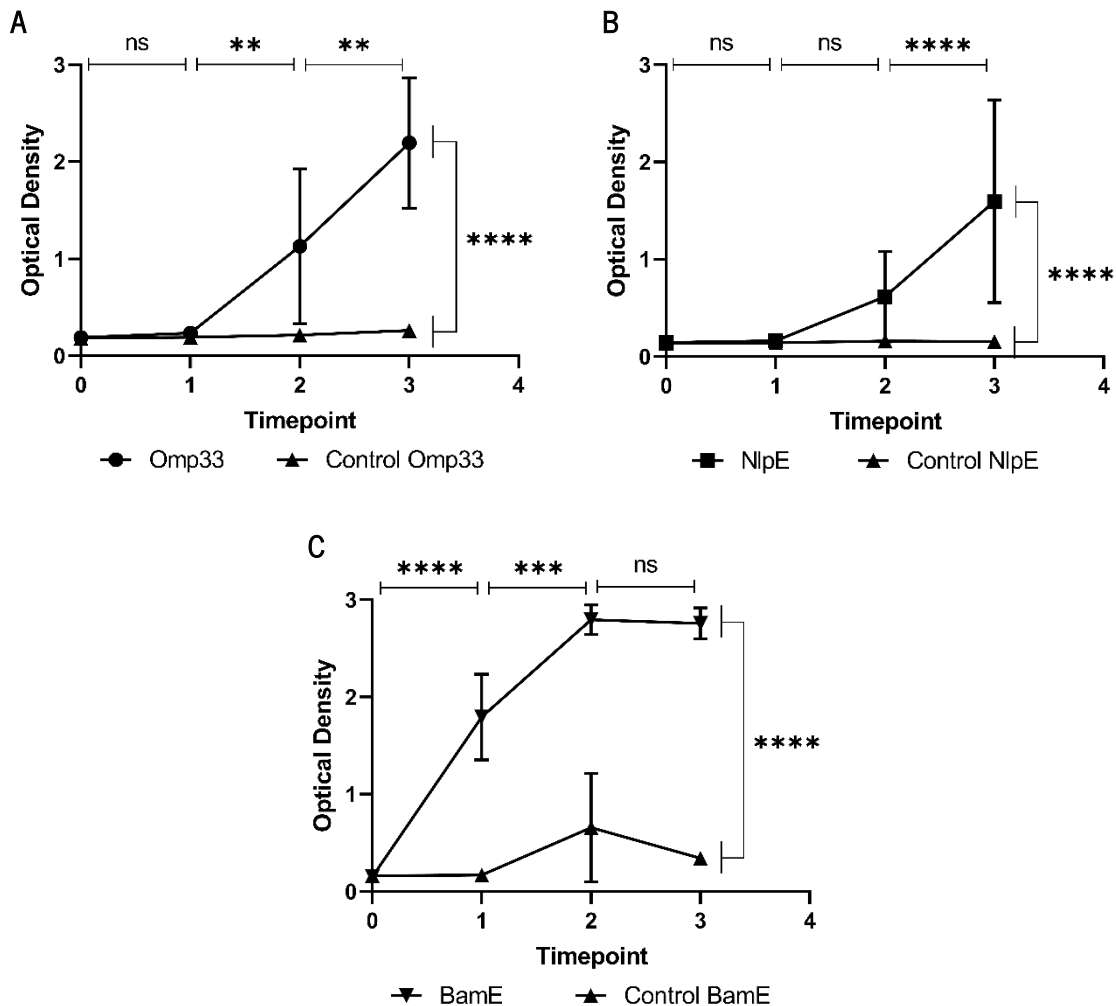
Figure 10 – Antibody production from immunization with proteins Omp33 (A), NlpE (B) and BamE (C). Results obtained by ELISA. The value of optical density is proportional to the amount of antibodies produced by the mice. The production of antibody was compared between timepoints, and the amount of antibodies produced after the three immunizations was compared to the control mice at the same timepoint. The asterisks represent the significance of the values being ****, pvalue < 0.0001; ***, pvalue = 0.0002; **, pvalue < 0.0040, and ns, not significant.

In general, all proteins induced a strong humoral immune response, especially by the third immunization. As mentioned, Omp33 protein had already been described as an immunogen [45],

which was confirmed by this study. Furthermore, the production of antibodies is the confirmation that the pipeline designed was successful in filtering potential immunogenic proteins.

For Omp33 protein, antibody production was significant after the second immunization, and further increased after the third administration. By its turn, immunization with NlpE only resulted in significant antibody production after the third inoculation, while immunization with BamE resulted in a significant production of antibodies immediately after the first inoculation and increased after the second.

Sera of the control group was compared to the sera of mice immunized with the proteins studied. Overall, antibodies against the immunogenic proteins were not present in the serum of control mice and the use of the adjuvant did not influence the production of specific antibodies against the proteins Omp33, NlpE and BamE. In addition, in every case, the amount of antibodies obtained by the end of the trial was significantly higher compared to the control, validating the immunogenic potential of the proteins.

As already mentioned, the Omp33 protein was used as proof-of-concept, given its already described immunogenic potential. Therefore, the level of antibodies produced of each study group was compared to Omp33, as shown in **Figure 11**, with no significative difference between Omp33 and NlpE, and between Omp33 and BamE. However, there was a significant difference between the induction from NlpE and BamE, being the last the one with a higher immunogenic potential.
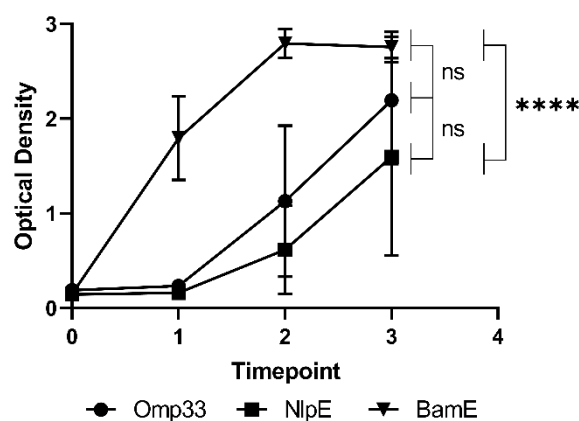
Figure 11 – Variation between proteins Omp33, NlpE and BamE antibody production.

The approach used to analyze the amount of antibodies produced only shows a value of optical density. To calculate the exact number of antibodies, a calibration curve should have been performed. However, for this, the number of antibodies against each protein should have been purified, quantified, and diluted to make the calibration curve for each one. Nevertheless, all

samples were analyzed in the same day, under the same conditions, to minimize variations. Since there are no exact value of antibodies, the results here obtained cannot be compared to the ones already published (**Table 1**).

Regarding protein BamE, a BLAST evaluation revealed the existence of a homolog protein in *Enterobacter asburiae*, which, although not present in human gut flora, is present in mice's gut [90]. Proteins from gut bacteria could be present as remnants in the blood and reach the liver, where there is, usually, an immunotolerance against gut-flora antigens. However, since we administered an adjuvant, which potentiates the immune response, the liver's immunotolerance might have been compromised, and consequently, there was a production of antibodies against the protein BamE. Besides, by inducing an immune response against a protein naturally present in mice, the production of antibodies against could be greater due the higher quantity of immunogen available in circulation, comparatively to the other proteins evaluated.

Ultimately, the proteins NlpE and BamE can be used in protein-based vaccines, after confirmation by further clinical trials. Still, this study has led to the finding of two novel immunogenic proteins against *A. baumannii*.

Histology

To develop a vaccine, it is necessary to assess more than just whether antibodies against the selected antigen were produced or not. To ensure its safety, it is also essential to assess any potential immunopathologic effect that the foreign body has on different organs. Considering this, it was decided to evaluate the effect of immunization on the spleen, and liver. The spleen is a secondary lymphoid organ that promotes the interaction between antigen-bearing innate immune cells and adaptive immune cells. As mentioned above, APCs can migrate to the spleen, where B-cells and T-cells are activated, inside specific structures known as germinal centers. B cells then initiate their differentiation into highly specific and high affinity antibody-producing plasmoblasts [91]. The liver, on the other hand, is a critical organ involved in blood filtration processes and catabolization of molecules present in the blood. Thus, we intend to assess whether histopathological changes could be observed in the organs of immunized mice when compared to vehicle-controls.

The histological evaluation of the organs by microscopy (**Figure 12**) proved that the administration of the proteins and with the adjuvant did not lead to histological changes in either the spleen or liver, since in none of the situations was it visible considerable differences in the cells'

structure and distribution, when compared to the control group. In the spleen, it was maintained the organized structure with a clear distinction between white pulp vs red pulp, with surrounding splenic sinusoids. Meanwhile, in the liver is visible an organized structure in which it is evident the presence of hepatocytes and Kupfer cells, with scattered blood vessels. Overall, in either case, no evidence of increased cell death or necrosis was observed.

The only outlier detected was the presence of inflammatory infiltrate in the liver of one mouse inoculated with the BamE, from a group of seven mice (data not shown). Nevertheless, it possible to conclude that there was no pathological effect from the inoculation with the proteins.
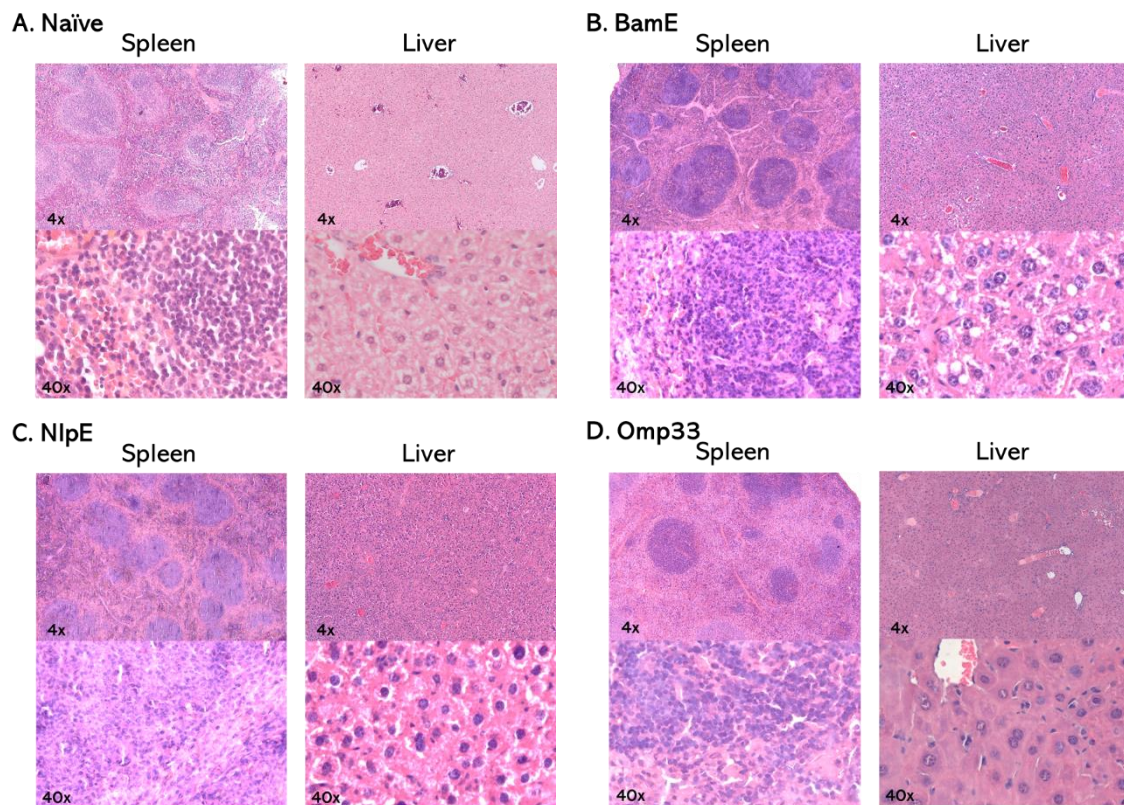

Figure 12 – Histology results. Herein are shown slides representative of the groups Naïve, BamE, NlpE and Omp33, for spleen and liver. The pictures are shown in the amplifications of 4x and 40x, as labelled.

3.3. Virulence Evaluation

To establish a possible correlation between the immunogenicity of the proteins and its virulence role in the bacteria, three mutants were constructed in *A. baumannii* ATCC 17978 strain: *Δomp33*, *ΔnlpE* *ΔbamE*. Next, these mutants were evaluated regarding their growth kinetics, biofilm formation and evasion of host immunity and compared with the wild-type strain.

Mutants' construction

When cells expressing *cas9* and recombinase were co-transformed with the sgRNA with targeting spacers and the donor DNA, different surviving bacterial colonies were observed. To facilitate comparisons between positive (with sgRNA with targeting spacers) and negative controls (with sgRNA without targeting spacers) with the recovered cells, i.e., all cells were diluted and plated, as exemplified in **Figure 13**.
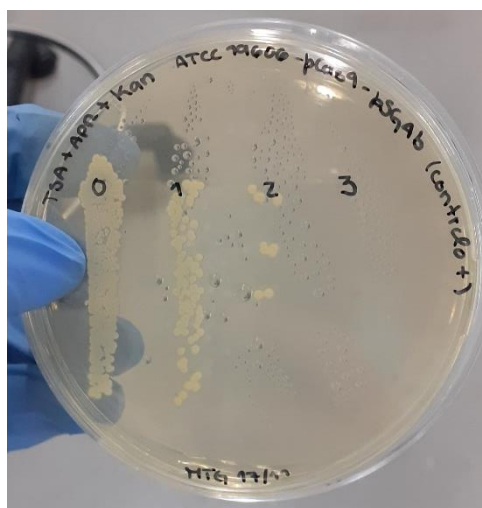
Figure 13 – Example of plated colonies for evaluation of mutant's growth. In this figure is shown a plate grown for the positive control. All plates were plated with 10 µL of each dilution and 10 µL of the mother culture.

Overall, there was a reduction of CFU's by four to five logs, while there was a recovery of usually one to two logs. These data allow us to conclude that the spacers were properly constructed. However, some attempts would not show a large reduction and therefore the mutants obtained would not be reliable. When there wasn't a big reduction, the mutant's gene could have been repaired trough the donor DNA, through endogenous mechanisms or there was no cleavage of the gene at the first place. When this happened, the amount of spacer would be later increased to

provoke a higher killing rate, and therefore reliable results.

Subsequently, $\Delta Omp33$, $\Delta NlpE$ and $\Delta BamE$ mutant candidates were confirmed by colony PCR gels (**Figure 14**).
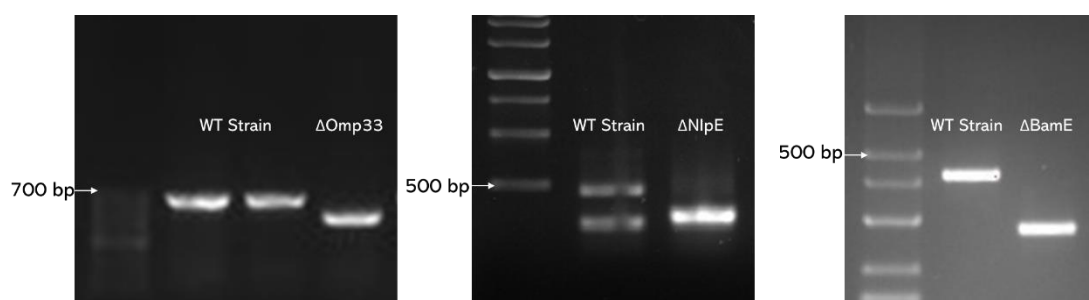
Figure 14 – Genome edition with CRISPR-CAS9. Agarose gels from the colony PCRs, showing the mutants $\Delta Omp33$, $\Delta nlpE$ and $\Delta bamE$, respectively. For both the mutants $\Delta omp33$ and $\Delta nlpE$, there was a decrease of about 183 bp, while for the $\Delta bamE$ mutant there was a decrease of about 145 bp. As a negative control, the colony PCRs was performed also for a colony of the WT strain, so the decrease of the gene size would be directly visualized in the gel.

As previously explained, understanding the biology of the pathogenic microorganism and its virulence factors is essential for the development of new therapeutic techniques. These virulence factors include secreted products or even structures present on the cell surface. Outer membrane proteins have a variety of functions in the cell, like maintaining the membrane structure and transportation (Xu et al., 2020). The genes that we have deleted encode outer membrane proteins which might be involved in the virulence. Omp33 has already been shown to participate in virulence. BamE, an outer membrane assembly factor, and NlpE, a copper resistant protein, are both present on the outer membrane and might also be involved in *A. baumannii*'s virulence as well. Thus, we intended to evaluate the $\Delta omp33$, $\Delta nlpE$ and $\Delta bamE$ mutants' ability to 1) grow in liquid media, 2) to form biofilms, and 3) to evade host immunity, comparatively to the WT strain. This would allow a direct relation between the proposed correlation among protein immunogenicity and virulence.

Virulence Assays

The ability of *A. baumannii* to adapt to the ambient and to resist adverse environmental challenges is the main factor for its pathogenicity [92]. Despite the research done, little is known about the virulence factors that support its pathogenicity and virulence, and as mentioned in chapter 1. The colonization of *A. baumannii* on human skin and on inert surfaces is related to the infection,

spread and persistence of this bacteria in the environment [10]. Destruction of epithelial cells can lead to the reduction of the mucosal surface and provide a pathway for deep tissue infection, either for the bacteria itself or for compounds produced by it [10,93,94].

Growth Assays

To understand if the removal of proteins (Omp33, NlpE and BamE) would influence their growth, we studied its growth curves and compared with the WT strain (**Figure 15**) Growth kinetics were also determined, such as the specific exponential growth rate, μ (h^{-1}), and the cell duplication time, Dt (h).
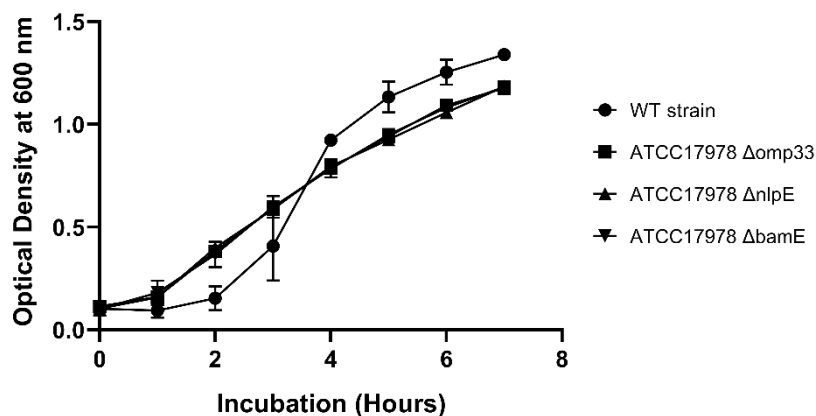
Figure 15 – WT and mutant's growth curves. The bacteria were grown in liquid medium, during 7 h of incubation.

Figure 15 shows that WT's growth curve had three different growth phases as expected during the 7 h of analysis (lag, exponential and stationary phase). Lag phase occurred between time points zero and two; exponential phase, between time points two and four, and the beginning of the stationary phase, after time point four. In turn, the mutants' growth curves, had indistinguishable growth phases. Nevertheless, we can limit the lag phase between the time points zero and one, the exponential growth between timepoints one and three, and finally, the stationary phase after the timepoint three. Comparatively to the WT strain, although the mutants shown a shorter lag stage, they never seem to reach growth values of optical density the WT reaches, and their exponential phase is not as accentuated as occurs in the WT.

From the linearization of the exponential phase identified, we obtained the values for μ and Dt, shown on **Table 5**.

Table 5 – Growth kinetics. Values for the exponential growth rate and for the duplication time, obtained for the WT strain and for each mutant.

	WT strain	Δomp33	ΔnlpE	ΔbamE
μ (h⁻¹)	0.862 ± 0.574	0.655 ± 1.901	0.659 ± 1.943	0.601 ± 0.269
Dt (h)	0.804 ± 0.124	1.058 ± 0.713	1.052 ± 0.722	1.154 ± 0.120

As shown on the table above, the WT strain as a higher growth rate than the mutants, meaning that the growth per hour is higher, which is confirmed by the value of the duplication time. This value is lesser than of the mutants, which means that the time it takes for the population to double is lesser for the WT than for the mutant strains.

Even though we can confirm that the absence of the proteins Omp33, NlpE and BamE alters the bacteria's growth, this assay should be performed during a longer time period, to correctly establish the stationary phase and the cell death decay and then compare the mutants and the WT. Nevertheless, through this assay it was possible to show that these proteins influence bacterial growth. One hypothesis is that the synthesis of the outer membrane is compromised during cell division. The bacteria may be developing secondary biochemical mechanisms to compensate for the weakening of the membrane, which means that there will be a greater consumption of energy diverted to other reactions, explaining a longer doubling time and a lower kinetic rate of growth. Since the mutants' growth differs from the WT's but not from between each other, this theory could explain this has an overall phenomenon, not dependent of each protein on itself, but has a trend resulting from the removal of a protein from the outer membrane.

Biofilm Assays

Biofilm formation by *A. baumannii* is vastly studied. Easy adherence to epithelial cells, to medical equipment and to devices is crucial for *A. baumannii* invasion of susceptible hosts. Thus, biofilms play an important role in the virulence of *A. baumannii* [11,94]. The bacterium's ability to colonize and produce biofilms contributes to chronic and persistent infections, antibiotic resistance, survival in hospitals and nosocomial infections [95,96]. *A. baumannii* presents a variety of virulence genes and regulatory networks of gene expression, involved in the formation of biofilms and their adhesion to surfaces [11,94,96].

By performing these assays, we intended to understand if the proteins Omp33, BamE and

NlpE engage in the development of biofilms by *A. baumannii* or if they alter its development. The values obtained for the formation of biofilms by the WT strain and the mutants are shown on the **Figure 16**.
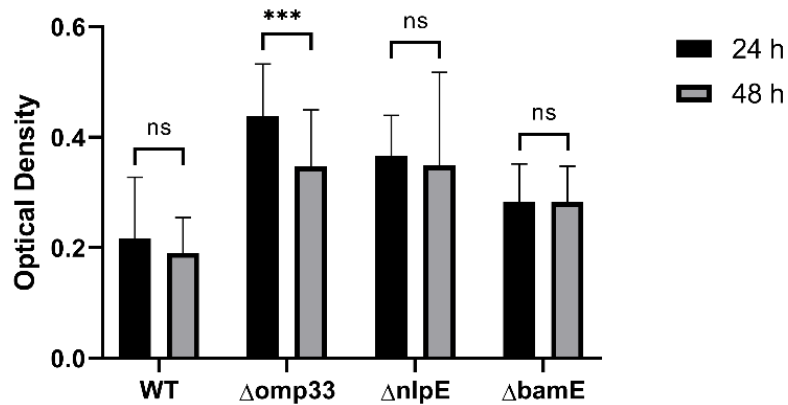
Figure 16 – Biofilm formation. Here are shown the growth values obtained after 24 and 48 h of growth. Biofilms were grown in 96-microtiter plates for 24 h, washed and stained with Crystal Violet. The asterisks represent the significance of the values being ****, pvalue < 0.0001 and ***, pvalue < 0.0003, and ns, not significant.

The figure shows the values of optical density, which are directly proportional to the amount of biofilm formed, for each mutant and for the WT strain, and their significance when compared to the WT. As visible, the formation of biofilms by the WT strain and by the mutants are significantly different, and, overall, all the mutants were able to produce more biofilms coupled to the plate wells than the WT strain.

Comparatively with the WT, the mutant *Δomp33* formed more biofilms. In one report, the *A. baumannii* mutant *Δomp33* had little to no significant differences when compared with the WT strain [97]. In contrast, a second report showed that *A. baumannii* mutant *Δomp33* made less biofilms than the WT [68]. Omp33 has long been reported has a virulence factor involved in resistance to carbapenems antibiotics, induction of apoptosis and overall the fitness of *A. baumannii* [68,98]. It also has been recently shown that it does not disable the adhesion ability of *A. baumannii* to surfaces [99] and, in the conditions tested here, it seems to in fact potentiate the adherence to the surface and formation of biofilms.

Comparing the mutant *ΔnlpE* and the WT strain, is also clear that the *ΔnlpE*'s biofilm formation was higher than the WT's. Studies on *E. coli* show that, although not directly and sole responsible, the NlpE has a significant role in the mediation of surface recognition and in the

stimulation of adherence [100,101], and in *A. baumannii* it was shown to have a similar role in sensing and inducing responses to different stressors, besides being involved in copper tolerance [102]. Considering these functions, it would be expected that the mutant lacking this protein would have a lesser ability to develop biofilms than the WT, however, in the conditions tested, its ability was significantly higher than the WT's, much like the case with the mutant *Δomp33*.

Comparing the mutant *ΔbamE* and the WT strain, it is, once again, noticeable that the mutant has developed more biofilms than the WT. Being an outer membrane assembly factor, BamE shows a role in defining the cell shape and in the outer membrane integrity, and enhances the biofilm formation [103], however, no data is documented if its absence reduces the biofilm development in *A. baumannii*. Indeed, looking at the data shown in the **Figure 16**, from all the three mutants, the *ΔbamE* shows the less amount of biofilm formation. Nevertheless, it still has a significantly higher production of biofilm than the WT strain.

Met with these results, it was proposed to perform this assay under the same conditions but for 48 h of growth, to understand the behaviour of the mutants after this time. The values obtained are shown on **Figure 16**. The added 24 h of growth was not significant for the formation of biofilms except for the Δomp33 mutant, that showed a decrease of biofilm. Still, all of the mutants were able to develop more biofilms than the WT.

Biofilms are formed on biotic and abiotic surfaces and consist of a matrix of carbohydrates, nucleic acids, proteins, and other macromolecules which protect the colony from damage caused by the surrounding environment such as host immune responses, antibiotics, detergents, or disinfectants [10,11,104]. Hypothetically, by removing outer membrane proteins the cell would be weakened, and therefore the formation of biofilms would be valuable for the colony survival due the shielding advantages. Therefore, the results here obtained could have resulted from a feedback mechanism of up-regulation gene transcription to develop more biofilms and protect the colonies.

Furthermore, the formation and regulation of biofilms depends on several environmental factors, such as growth conditions, cell density, quorum sensing, light availability, free iron, surface porosity, fluid flow and nutrient availability [11,96]. The biofilm development is controlled by quorum sensing and comprises three main stages: the initial contact and adhesion, the maturation and formation of the biofilm architecture, and the separation of the biofilm from the surface [96]. In this study, we have only evaluated the biofilm formation controlling the temperature, agitation, and time. Several other factors were out of our control, such has light availability and fluid flow. To understand the impact of the removal of the proteins Omp33, NlpE and BamE in biofilm

development and their implications in medical devices and epithelial cells, more specific studies should be conducted. It is also proposed to take samples of the adhered biofilm at different timepoints and plate them in order to evaluate the biofilm's viability. Since biofilms of this bacteria are very usual in medical devices, it would be valuable to understand if the mutants would still be able have the same characteristics as before and the same ability to infect epithelial cells.

Human serum Assays

In 2017, Sanchez-Larrayoz and colleagues have identified 50 genes essential for the survival of *A. baumannii* in normal human serum and observed that serum resistance is a common feature among virulent *A. baumannii* strains. Additionally, it was shown that human serum albumin plays a significant role in survival and persistence of *A. baumannii* in human serum [106].

To understand if there is any influence of the absence of Omp33, NlpE and BamE in the survival of *A. baumannii* in contact with human serum, the mutants and the WT were incubated with serum from healthy volunteers, and the survival bacteria was evaluated by CFU counting (**Figure 17**).
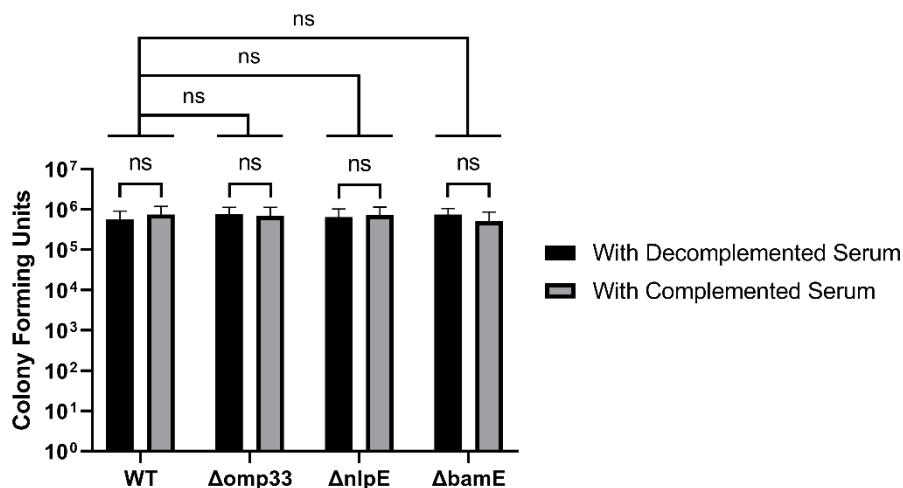
Figure 17 – Serum assay. Cells (WT and mutants) were incubated with human serum complemented and decomplemented (heat-inactivated) for one hour. After incubation CFUs were obtained and compared. Here is shown the significance between survival with each of the serums and between each strain. ns: not significant.

Results showed that there is no significant difference between the ability of the WT and mutants to evade the host complement. Thus, we can conclude that these proteins are not essential for the survival of the bacteria in normal human serum, which is confirmed by Sanchez-

Larrayoz and colleagues [105]. From the fifty essential genes identified by them, none were the ones studied here or homologs, whereby, the absence of these genes does not alter the bacteria's survival when in contact with human serum.

Even so, it was possible to notice that after contact with the serum, the mutant colonies exhibited different morphology than the WT, appearing smaller in diameter, as shown in **Figure 18**.
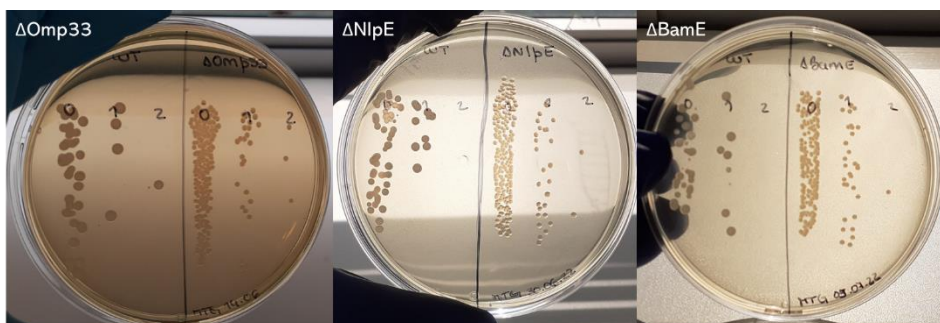
Figure 18 – CFU grown after incubation with normal human serum for each mutant Δomp33, ΔnlpE and ΔbamE. For each situation is also shown in the same plate the CFU of the WT strain for the same conditions. Additionally, for each one is shown two dilutions.

Globally, these three assays allowed us to recognize some differences between the mutants and the WT, and conclude that the absence of the proteins Omp33, NlpE and BamE, does affect the fitness of *A. baumannii*, however, it does not alter the bacteria's ability to form biofilms neither influences its survival against human serum. Unlike other immunogenic proteins tested in *A. baumannii* which are related to virulence factors (like OmpA[86,107,108], Phospholipase D[84,109] and Omp33[68,98]), the proteins NlpE and BamE do not show this to be so. Since these proteins are present in the outer membrane, it was expected that their removal would reduce the bacterial virulence, justifying in part the lower growth rate obtained. Possibly, to confirm the virulence role of these genes other assay would need to be performed, such as adherence/evasion of mammalian assays.

The definition of virulence varies among different disciplines and little consensus exists regarding its distinction from pathogenicity. Nevertheless, virulence is often described as the impact of the pathogen on the fitness of infected hosts. Regardless, infectivity, virulence and pathogenicity are considered properties of the pathogen, but measured considering the response of the host, according to the environment that they are in [110].

Although these assays allowed us to understand the alteration of some factors between the mutants and the WT, the evaluation of these mutants in *in vivo* assays would give a better understanding of the implications of removing these proteins from the membrane, and fully

understand the shifts between the bacteria's virulence and pathogenicity and if there is in fact a direct relationship between immunogenicity and virulence

CHAPTER 4

Conclusions and Future Perspectives

4.1. Conclusions

Overall, the main objectives of the present work were to develop a pipeline to identify proteins with immunogenic potential against *A. baumannii*; to test their immunogenicity *in vivo* and, additionally, to test whether the selected immunogenic proteins were somehow involved in the virulence of *A. baumannii* or not. In general, we can confirm that the first two objectives were successfully achieved, while the third should be further assessed to draw final conclusions.

Regarding the pipeline developed, although the immunoinformatics tool applied was unsuccessful, but the filtration performed by reverse vaccinology was effective in sorting membrane proteins with immunogenic potential, of which a few had already been described in the literature or demonstrated in this work. One of the main achievements was the prediction soluble protein vaccine candidates, frequently reported in literature as insoluble, benefiting the large-scale production of more affordable recombinant vaccines. In fact, inoculation of mice with the proteins Omp33, NlpE and BamE resulted in the induction of an immune response and in antibody production. Additionally, there weren't found changes at the cellular level in the organs studied here, whereby we can assume that the inoculation of these proteins had no pathological effects. Although the Omp33 protein has already been indicated as an immunogenic protein, here it was administered to function as a baseline for the data. Comparing the NlpE and BamE proteins with Omp33, we can verify that the values obtained are very similar, both in terms of antibody production and in terms of histology, so we can confirm that the NlpE and BamE were successfully produced as soluble recombinant proteins with high immunogenic potential.

Regarding the role virulence role of Omp33, BamE and NlpE, the results did not allow us to reach significant conclusions. In fact, the absence of these proteins in bacteria affects the general fitness of *A. baumannii*. However, to conclude whether the proteins are indeed linked to virulence or not, more specific tests should be carried out and also in animal models.

4.2. Future Perspectives

Despite of this work being concluded, there are still trials that can strengthen the conclusions achieved here. Thus, for the validation of the NlpE and BamE proteins as immunogenic proteins, we propose the replication of the *in vivo* assays, increasing the number of animals tested

and testing the efficiency of memory immunity, via infection of the mice with the bacterium and analysis of the mice's survival and the immune system response of vaccinated versus unvaccinated mice.

Regarding the evaluation of virulence of mutants lacking BamE and NlpE proteins, it is suggested to carry out virulence assays in invertebrate models such as *Caenorhabditis elegans* or *Galleria mellonella*, to analyze the survival rate after infection with WT versus mutants.

REFERENCES

References

1. Sengupta, S., Chattopadhyay, M. K. & Grossart, H. The multifaceted roles of antibiotics and antibiotic resistance in nature. *Front. Microbiol.* **4**, 47 (2013).

2. Ventola, C. L. The antibiotic resistance crisis: part 1: causes and threats. *P T a peer-reviewed J. Formul. Manag.* **40**, 277–283 (2015).

3. Santajit, S. & Indrawattana, N. Mechanisms of Antimicrobial Resistance in ESKAPE Pathogens. *Biomed Res. Int.* **2016**, 2475067 (2016).

4. de Kraker, M. E. A., Stewardson, A. J. & Harbarth, S. Will 10 Million People Die a Year due to Antimicrobial Resistance by 2050?. *PLoS Med.* **13**, e100218 (2016).

5. Rios, A. C. *et al.* Alternatives to overcoming bacterial resistances: state-of-the-art. *Microbiol. Res.* **181**, 51–80 (2016).

6. Pendleton, J. N., Gorman, S. P. & Gilmore, B. F. Clinical relevance of the ESKAPE pathogens. *Expert Rev. Anti. Infect. Ther.* **11**, 297–308 (2013).

7. Lee, C.-R. *et al.* Biology of *Acinetobacter baumannii*: Pathogenesis, Antibiotic Resistance Mechanisms, and Prospective Treatment Options. *Front. Cell. Infect. Microbiol.* **7**, 55 (2017).

8. Moubareck, C. A. & Halat, D. H. Insights into *Acinetobacter baumannii*: A Review of Microbiological, Virulence, and Resistance Traits in a Threatening Nosocomial Pathogen. *Antibiot. (Basel, Switzerland)* **9**, 119 (2020).

9. Vázquez-López, R. *et al. Acinetobacter baumannii* Resistance: A Real Challenge for Clinicians. *antibiotics* **9**, 1–22 (2020).

10. Ibrahim, S., Al-Saryi, N., Al-Kadmy, I. M. S. & Aziz, S. N. Multidrug-resistant *Acinetobacter baumannii* as an emerging concern in hospitals. *Mol. Biol. Rep.* **48**, 6987–6998 (2021).

11. Kumar, S., Anwer, R. & Azzi, A. Virulence potential and treatment options of multidrug-resistant (MDR) *Acinetobacter baumannii. Microorganisms* **9**, 2104 (2021).

12. Abedon, S. T., Kuhl, S. J., Blasdel, B. G. & Kutter, E. M. Phage treatment of human infections. *Bacteriophage* **1**, 66–85 (2011).

13. Mulani, M. S., Kamble, E. E., Kumkar, S. N., Tawre, M. S. & Pardesi, K. R. Emerging Strategies to Combat ESKAPE Pathogens in the Era of Antimicrobial Resistance: A Review. *Front. Microbiol.* **10**, 539 (2019).

14. Isler, B., Doi, Y., Bonomo, R. A. & Paterson, D. L. New Treatment Options against

Carbapenem-Resistant *Acinetobacter baumannii* Infections. *Antimicrob. Agents Chemother.* **63**, e01110-18 (2019).

15. Baginska, N., Pichlak, A., Górski, A. & Jonczyk-Matysiak, E. Specific and Selective Bacteriophages in the Fight against Multidrug-resistant *Acinetobacter baumannii*. *Virol. Sin.* **34**, 347–357 (2019).

16. Bochkareva, S. *et al.* Anti-phage antibody response in phage therapy against healthcare-associated infections (HAIs). *Infekc. Bolezn. (Infectious Dis.* **15**, 35–40 (2017).

17. Ghajavand, H. *et al.* Isolation of bacteriophages against multidrug resistant *Acinetobacter baumannii*. *Res. Pharm. Sci.* **12**, 371–380 (2017).

18. Schooley, R. T. *et al.* Development and Use of Personalized Bacteriophage-Based Therapeutic Cocktails To Treat a Patient with a Disseminated Resistant *Acinetobacter baumannii* Infection. *Antimicrob. Agents Chemother.* **61**, e00954-17 (2017).

19. Turner, D. *et al.* Characterisation and genome sequence of the lytic *Acinetobacter baumannii* bacteriophage vB_AbaS_Loki. *PLoS One* **12**, e0172303 (2017).

20. Lood, R. *et al.* Novel phage lysin capable of killing the multidrug-resistant gram-negative bacterium *Acinetobacter baumannii* in a mouse bacteremia model. *Antimicrob. Agents Chemother.* **59**, 1983–1991 (2015).

21. Knirel, Y. A. *et al.* Mechanisms of *Acinetobacter baumannii* Capsular Polysaccharide Cleavage by Phage Depolymerases. *Biochemistry. (Mosc).* **85**, 567–574 (2020).

22. Oliveira, H. *et al.* Functional Analysis and Antivirulence Properties of a New Depolymerase from a Myovirus That Infects *Acinetobacter baumannii* Capsule K45. *J. Virol.* **93**, e01163-18 (2019).

23. Wang, C. *et al.* Identification of a Novel *Acinetobacter baumannii* Phage-Derived Depolymerase and Its Therapeutic Application in Mice. *Front. Microbiol.* **11**, 1407 (2020).

24. Shahed-Al-Mahmud, M. *et al.* Phage фab6-borne depolymerase combats *Acinetobacter baumannii* biofilm formation and infection. *Antibiot. (Basel, Switzerland)* **10**, 279 (2021).

25. Brandenburg, L., Merres, J., Albrecht, L., Varoga, D. & Pufe, T. Antimicrobial Peptides: Multifunctional Drugs for Different Applications. *Polymers (Basel).* **4**, 539–560 (2012).

26. Peng, J. *et al.* Antibacterial mechanism of peptide Cec4 against *Acinetobacter baumannii*. *Infect. Drug Resist.* **12**, 2417–2428 (2019).

27. Jung, C. J. *et al.* Identification of potential therapeutic antimicrobial peptides against *Acinetobacter baumannii* in a mouse model of pneumonia. *Sci. Rep.* **11**, 7318 (2021).

28. Guimarães, L. E., Baker, B., Perricone, C. & Shoenfeld, Y. Vaccines, adjuvants and autoimmunity. *Pharmacol. Res.* **100**, 190–209 (2015).

29. Baxter, D. Active and passive immunity, vaccine types, excipients, and licensing. *Occup. Med. (Lond).* **57**, 552–556 (2007).

30. Pavia, C. S. & Wormser, G. P. Passive immunization and its rebirth in the era of the COVID-19 pandemic. *Int. J. Antimicrob. Agents* **57**, 106275 (2021).

31. Ellis, R. W., Rappuoli, R. & Ahmed, S. *Technologies for making new vaccines. Vaccines* (Elsevier Inc., 2013). doi:10.1016/B978-1-4557-0090-5.00013-6

32. Francis, M. J. Recent Advances in Vaccine Technologies. *Vet. Clin. North Am. Small Anim. Pract.* **48**, 231–241 (2018).

33. Piyush, R., Rajarshi, K., Chatterjee, A., Khan, R. & Ray, S. Nucleic acid-based therapy for coronavirus disease 2019. *Heliyon* **6**, e05007 (2020).

34. Silveira, M. M., Moreira, G. & Mendonça, M. DNA vaccines against COVID-19: Perspectives and challenges. *Life Sci.* **267**, 118919 (2021).

35. Tsoras, A. N. & Champion, J. A. Protein and Peptide Biomaterials for Engineered Subunit Vaccines and Immunotherapeutic Applications. *Annu. Rev. Chem. Biomol. Eng.* **10**, 337–359 (2019).

36. MacRaild, C. A., Seow, J., Das, S. C. & Norton, R. S. Disordered epitopes as peptide vaccines. *Pept. Sci. (Hoboken, N.J.)* **110**, e24067 (2018).

37. Moyer, T. J., Zmolek, A. C. & Irvine, D. J. Beyond antigens and adjuvants: formulating future vaccines. *J. Clin. Invest.* **126**, 799–808 (2016).

38. Chiang, M. *et al.* Identification of novel vaccine candidates against *Acinetobacter baumannii* using reverse vaccinology. *Hum. Vaccin. Immunother.* **11**, 1065–1073 (2015).

39. Singh, R., Capalash, N. & Sharma, P. Immunoprotective potential of BamA, the outer membrane protein assembly factor, against MDR *Acinetobacter baumannii*. *Sci. Rep.* **7**, 12411 (2017).

40. Li, H. *et al.* Small protein A and phospholipase D immunization serves a protective role in a mouse pneumonia model of *Acinetobacter baumannii* infection. *Mol. Med. Rep.* **16**, 1071–1078 (2017).

41. Luo, G. *et al.* Active and passive immunization protects against lethal, extreme drug resistant-*Acinetobacter baumannii* infection. *PLoS One* **7**, e29446 (2012).

42. Rasooli, I., Abdolhamidi, R., Jahangiri, A. & Astaneh, S. D. A. Outer Membrane Protein,

Oma87 Prevents *Acinetobacter baumannii* Infection. *Int. J. Pept. Res. Ther.* **26**, 2653–2660 (2020).

43. Bentancor, L. V *et al.* Evaluation of the trimeric autotransporter Ata as a vaccine candidate against *Acinetobacter baumannii* infections. *Infect. Immun.* **80**, 3381–3388 (2012).

44. Fattahian, Y. *et al.* Protection against *Acinetobacter baumannii* infection via its functional deprivation of biofilm associated protein (Bap). *Microb. Pathog.* **51**, 402–406 (2011).

45. Erami, A. N., Rasooli, I., Jahangiri, A. & Astaneh, S. D. A. Microbial Pathogenesis Anti-Omp34 antibodies protect against *Acinetobacter baumannii* in a murine sepsis model. *Microb. Pathog.* **161**, 105291 (2021).

46. Abdollahi, S., Raoufi, Z. & Fakoor, M. H. Physicochemical and structural characterization, epitope mapping and vaccine potential investigation of a new protein containing Tetratrico Peptide Repeats of *Acinetobacter baumannii*: An in-silico and in-vivo approach. *Mol. Immunol.* **140**, 22–34 (2021).

47. Avci, F. *et al.* Glycoconjugates: What It Would Take To Master These Well-Known yet Little-Understood Immunogens for Vaccine Development. *mSphere* **4**, e00520-19 (2019).

48. Rappuoli, R. Glycoconjugate vaccines: Principles and mechanisms. *Sci. Transl. Med.* **10**, eaat4615 (2018).

49. Tontini, M. *et al.* Preclinical studies on new proteins as carrier for glycoconjugate vaccines. *Vaccines* **34**, 4235–4242 (2016).

50. Müller, L., Benedetto, S. & Pawelec, G. The Immune System and Its Dysregulation with Aging. *Subcell. Biochem.* **91**, 21–43 (2019).

51. Nicholson, L. B. The immune system. *Essays Biochem.* **60**, 275–301 (2016).

52. Netea, M. G., Schlitzer, A., Placek, K., Joosten, L. & Schultze, J. L. Innate and Adaptive Immune Memory: an Evolutionary Continuum in the Host's Response to Pathogens. *Cell Host Microbe* **25**, 13–26 (2019).

53. Hato, T. & Dagher, P. C. How the Innate Immune System Senses Trouble and Causes Trouble. *Clin. J. Am. Soc. Nephrol.* **10**, 1459–1469 (2015).

54. Kaur, B. P. & Secord, E. Innate Immunity. *Pediatr. Clin. North Am.* **66**, 905–911 (2019).

55. Zinsli, L. V., Stierlin, N., Loessner, M. J. & Schmelcher, M. Deimmunization of protein therapeutics - Recent advances in experimental and computational epitope prediction and deletion. *Comput. Struct. Biotechnol. J.* **19**, 315–329 (2021).

56. Sauls, R. S., McCausland, C. & Taylor, B. N. *Histology, T-Cell Lymphocyte*. (StatPearls

Publishing, 2021).

57. Almeida, L., Dhillon-labrooy, A., Carriche, G., Berod, L. & Sparwasser, T. CD4+ T-cell differentiation and function: Unifying glycolysis, fatty acid oxidation, polyamines NAD mitochondria. *J. Allergy Clin. Immunol.* **148**, 16–32 (2021).

58. Yatim, K. M. & Lakkis, F. G. A brief journey through the immune system. *Clin. J. Am. Soc. Nephrol.* **10**, 1274–1281 (2015).

59. Sanchez-Trincado, J. L., Gomez-Perosanz, M. & Reche, P. A. Review Article Fundamentals and Methods for T- and B-Cell Epitope Prediction. *J. Immunol. Res.* **2017**, 2680160 (2017).

60. Rizwan, M. *et al.* VacSol: a high throughput in silico pipeline to predict potential therapeutic targets in prokaryotic pathogens using subtractive reverse vaccinology. *BMC Bioinformatics* **18**, 106 (2017).

61. Dhanda, S. K. *et al.* Novel in silico tools for designing peptide-based subunit vaccines and immunotherapeutics. *Brief. Bioinform.* **18**, 467–478 (2017).

62. Dhanda, S. K. *et al.* IEDB-AR: immune epitope database-analysis resource in 2019. *Nucleic Acids Res.* **47**, W502–W506 (2019).

63. Pontes, G. D. M., Fernandes, L. S., Vander, R. V. dos, Tasic, L. & Fill, T. P. Virulence Factors in the Phytopathogen – Host Interactions : An Overview. *J. Agric. Food Chem.* **68**, 7555–7570 (2020).

64. Leitão, J. H. Microbial Virulence Factors. *Int. J. Mol. Sci.* **21**, 5320 (2020).

65. Moubareck, C. A. & Halat, D. H. Insights into *Acinetobacter baumannii*: A Review of Microbiological, Virulence, and Resistance Traits in a Threatening Nosocomial Pathogen. *Antibiot. (Basel, Switzerland)* **9**, 119 (2020).

66. Xu, C., Soyfoo, D. M., Wu, Y. & Xu, S. Virulence of *Helicobacter pylori* outer membrane proteins: an updated review. *Eur. J. Clin. Microbiol. Infect. Dis. Off. Publ. Eur. Soc. Clin. Microbiol.* **39**, 1821–1830 (2020).

67. Smani, Y., McConnell, M. J. & Pachón, J. Role of fibronectin in the adhesion of *Acinetobacter baumannii* to host cells. *PLoS One* **7**, e33073 (2012).

68. Smani, Y., Dominguez-Herrera, J. & Pachón, J. Association of the outer membrane protein Omp33 with fitness and virulence of *Acinetobacter baumannii*. *J. Infect. Dis.* **208**, 1561–1570 (2013).

69. Whiteside, M. D., Winsor, G. L., Laird, M. R. & Brinkman, F. S. OrtholugeDB: a bacterial and archaeal orthology resource for improved comparative genomic analysis. *Nucleic Acids*

Res. **41**, D366–D376 (2013).

70.   Xu, L. *et al.* OrthoVenn2: a web server for whole-genome comparison and annotation of orthologous clusters across multiple species. *Nucleic Acids Res.* **47**, W52–W58 (2019).

71.   He, Y., Xiang, Z. & Mobley, H. L. Vaxign: the first web-based vaccine design program for reverse vaccinology and applications for vaccine development. *J. Biomed. Biotechnol.* **2010**, (2010).

72.   Soltan, M. A., Magdy, D., Solyman, S. M. & Hanora, A. Design of *Staphylococcus aureus* New Vaccine Candidates with B and T Cell Epitope Mapping, Reverse Vaccinology, and Immunoinformatics. *OMICS* **24**, 195–204 (2020).

73.   Yu, N. Y. *et al.* PSORTb 3.0: improved protein subcellular localization prediction with refined localization subcategories and predictive capabilities for all prokaryotes. *Bioinformatics* **26**, 1608–1615 (2010).

74.   Remmert, M., Linke, D., Lupas, A. N. & Söding, J. HHomp–prediction and classification of outer membrane proteins. *Nucleic Acids Res.* **37**, W446–W451 (2009).

75.   Krogh, A., Larsson, B., von Heijne, G. & Sonnhammer, E. L. Predicting transmembrane protein topology with a hidden Markov model: application to complete genomes. *J. Mol. Biol.* **305**, 567–580 (2001).

76.   Magnam, C. N., Randall, A. & Baldi, P. SOLpro: accurate sequence-based prediction of protein solubility. *Bioinformatics* **25**, 2200–2207 (2009).

77.   Wang, Y., Wang, Z. & Ji, Q. CRISPR-Cas9-Based Genome Editing and Cytidine Base Editing in *Acinetobacter baumannii*. *STAR Protoc.* **1**, 100025 (2020).

78.   Srivastava, V., Mishra, S. & Chaudhuri, T. K. Enhanced production of recombinant serratiopeptidase in *Escherichia coli* and its characterization as a potential biosimilar to native biotherapeutic counterpart. *Microb. Cell Fact.* **18**, 215 (2019).

79.   McGuffin, L. J., Bryson, K. & Jones, D. T. The PSIPRED protein structure prediction server. *Bioinformatics* **16**, 404–405 (2000).

80.   Pires, D. P. *et al.* A Genotypic Analysis of Five *P. aeruginosa* Strains after Biofilm Infection by Phages Targeting Different Cell Surface Receptors. *Front. Microbiol.* **8**, 1229 (2017).

81.   Shahid, F., Ashraf, S. T. & Ali, A. Reverse Vaccinology Approach to Potential Vaccine Candidates Against *Acinetobacter baumannii*. *Methods Mol. Biol.* **1946**, 329–336 (2019).

82.   Bonin, R. F. *et al.* Identification of immunogenic proteins of the bacterium *Acinetobacter baumannii* using a proteomic approach. *Proteomics. Clin. Appl.* **8**, 916–923 (2014).

83. Jensen, K. K. *et al.* Improved methods for predicting peptide binding affinity to MHC class II molecules. *Immunology* **154**, 394–406 (2018).

84. Hosseingholi, E. Z., Rasooli, I. & Gargari, S. L. M. In Silico Analysis of *Acinetobacter baumannii* Phospholipase D as a Subunit Vaccine Candidate. *Acta Biotheor.* **62**, 455–478 (2014).

85. Hu, Y. Y. *et al.* Regulation of gene expression of hcp, a core gene of the type VI secretion system in *Acinetobacter baumannii* causing respiratory tract infection. *J. Med. Microbiol.* **67**, 945–951 (2018).

86. Nie, D. *et al.* Outer membrane protein A (OmpA) as a potential therapeutic target for *Acinetobacter baumannii* infection. *J. Biomed. Sci.* **27**, 26 (2020).

87. Gopal, G. J. & Kumar, A. Strategies for the Production of Recombinant Protein in *Escherichia coli*. *Protein J.* **32**, 419–425 (2013).

88. Miles, A. J., Janes, R. W. & Wallace, B. A. Tools and methods for circular dichroism spectroscopy of proteins: a tutorial review. *Chem. Soc. Rev.* **50**, 8400–8413 (2021).

89. Luo, J. *et al.* Targeted Inhibition of FTO Demethylase Protects Mice Against LPS-Induced Septic Shock by Suppressing NLRP3 Inflammasome. *Front. Immunol.* **12**, 663295 (2021).

90. Yang, J. & Chun, J. Taxonomic composition and variation in the gut microbiota of laboratory mice. *Mamm. Genome* **32**, 297–310 (2021).

91. Mebius, R. E. & Kraal, G. Structure and function of the spleen. *Nat. Rev. Immunol.* **5**, 606–616 (2005).

92. Antunes, L. C. S., Visca, P. & Towner, K. J. *Acinetobacter baumannii*: Evolution of a global pathogen. *Pathog. Dis.* **71**, 292–301 (2014).

93. Choi, C. H. *et al.* Outer membrane protein 38 of *Acinetobacter baumannii* localizes to the mitochondria and induces apoptosis of epithelial cells. *Cell. Microbiol.* **7**, 1127–1138 (2005).

94. Harding, C. M., Hennon, S. W. & Feldman, M. F. Uncovering the mechanisms of *Acinetobacter baumannii* virulence. *Nat. Rev. Microbiol.* **16**, 91–102 (2019).

95. Rodríguez-Baño, J. *et al.* Biofilm formation in *Acinetobacter baumannii*: associated features and clinical implications. *Clin. Microbiol. Infect.* **14**, 276–278 (2008).

96. Gedefie, A. *et al.* *Acinetobacter baumannii* biofilm formation and its role in disease pathogenesis: A review. *Infect. Drug Resist.* **14**, 3711–3719 (2021).

97. Cabral, M. P. *et al.* Proteomic and functional analyses reveal a unique lifestyle for

Acinetobacter baumannii biofilms and a key role for histidine metabolism. *J. Proteome Res.* **10**, 3399–3417 (2011).

98.   Rumbo, C. *et al.* The *Acinetobacter baumannii* Omp33-36 porin is a virulence factor that induces apoptosis and modulates autophagy in human cells. *Infect. Immun.* **82**, 4666–4680 (2014).

99.   Marazzato, M. *et al.* Genetic Diversity of Antimicrobial Resistance and Key Virulence Features in Two Extensively Drug-Resistant *Acinetobacter baumannii* Isolates. *Int. J. Environ. Res. Public Health* **19**, 2870 (2022).

100.   Otto, K. & Silhavy, T. J. Surface sensing and adhesion of *Escherichia coli* controlled by the Cpx-signaling pathway. *Proc. Natl. Acad. Sci. U. S. A.* **99**, 2287–2292 (2002).

101.   Lacanna, E., Bigosch, C., Kaever, V., Boehm, A. & Becker, A. Evidence for *Escherichia coli* diguanylate cyclase DgcZ interlinking surface sensing and adhesion via multiple regulatory routes. *J. Bacteriol.* **198**, 2524–2535 (2016).

102.   Kuo, H. Y. *et al.* Functional characterization of *Acinetobacter baumannii* Lacking the RNA chaperone Hfq. *Front. Microbiol.* **8**, 2068 (2017).

103.   Park, J. *et al.* A novel decoy strategy for polymyxin resistance in *Acinetobacter baumannii*. *Elife* **10**, e66988 (2021).

104.   Kim, H. R., Shin, D. S., Jang, H. I. & Eom, Y. Bin. Anti-biofilm and anti-virulence effects of zerumbone against *Acinetobacter baumannii*. *Microbiol. (United Kingdom)* **166**, 717–726 (2020).

105.   Sanchez-Larrayoz, A. F. *et al.* Complexity of Complement-Resistance Factors Expressed by *Acinetobacter baumannii* Needed for Survival in Human Serum. *J. Immunol.* **199**, 2803–2814 (2017).

106.   Quinn, B. *et al.* Human serum albumin alters specific genes that can play a role in survival and persistence in *Acinetobacter baumannii*. *Sci. Rep.* **8**, 14741 (2018).

107.   Davoudi, Z., Taromchi, A., Kazemi, B., Bandehpour, M. & Mosaffa, N. Cloning, expression, purification and functional analysis of a specific multi-epitope protein from multi drug resistance *Acinetobacter baumannii*. *Iran. J. Microbiol.* **13**, 642–652 (2021).

108.   Yang, C. H., Su, P. W., Moi, S. H. & Chuang, L. Y. Biofilm Formation in *Acinetobacter baumannii*: Genotype-Phenotype Correlation. *Molecules* **24**, 1849 (2019).

109.   Jacobs, A. C. *et al.* Inactivation of phospholipase D diminishes *Acinetobacter baumannii* pathogenesis. *Infect. Immun.* **78**, 1952–1962 (2010).

110. Thomas, S. R. & Elkinton, J. S. Pathogenicity and virulence. *J. Invertebr. Pathol.* **85**, 146–151 (2004).

ATTACHMENTS

Attachment I – Reverse Vaccinology and Immunoinformatics

Table 1 – *A. baumannii* strains selected for ortholog evaluation. The strains were selected from the ones made available by the OrtholugeDB program.

Bacterium	Strain
A. baumannii	1656-2
	AB0057
	AB307-0294
	ACICU
	AYE
	MDR-TJ
	MDR-2J06
	SDF
	TCDC-AB0715
	ATCC17978

Table 2 – HLA-Alleles chosen for MHC binding prediction.

Locus	MHC Allele
HLA-DR	β1*01:01
	β1*03:01
	β1*04:01
	β1*04:05
	β1*07:01
	β1*11:01
	β1*13:02

Table 3 – Reverse Vaccinology results.

Protein	Psortb 2.0 Localization	Vaxign Trans-membrane helices	Vaxign Adhesin Probability	Cusabio MW(kda)	Solpro prediction Solubility	Solpro prediction Probability
NZ_CP049363_-_outer_membrane_beta-barrel_protein, ompw homolog	Outermembrane	0	0,641	21,23	Soluble	0.962
NZ_CP049363_-_hypothetical_protein 67	Extracellular	0	0,827	27,67	Insoluble	0.892
NZ_CP049363_-_ompa_family_protein (ompa2)	Outermembrane	0	0,722	22,49	Soluble	0.536
NZ_CP049363_-_bame	Outermembrane	0	0,696	14,36	Soluble	0.539
NZ_CP049363_-_copper_resistance_protein_nlpe	Outermembrane	0	0,655	17,55	Soluble	0.934
NZ_CP049363_-_tetratricopeptide_repeat_protein 3	Extracellular	0	0,736	32,51	Soluble	0.708
NZ_CP049363_-_hypothetical_protein 322	Outermembrane	0	0,724	38,82	Soluble	0.522
NZ_CP049363_-_porin	Outermembrane	0	0,521	39,84	Insoluble	0.589
NZ_CP049363_-_type_VI_secretion_system_tube_protein_Hcp	Extracellular	0	0,72	18,75	Soluble	0.708

NZ_CP049363_-_peptidoglycan_DD-metalloendopeptidase_family_protein 2	Outermembrane	1	0,633	29,62	Insoluble	0.550
NZ_CP049363_-_pal	Outermembrane	0	0,663	20,08	Insoluble	0.950
NZ_CP049363_-_Plug_domain-containing_protein	Extracellular	0	0,699	25,57	Insoluble	0.699
NZ_CP049363_-_ompa-1_family_protein	Outermembrane	1	0,673	38,46	Insoluble	0.910
NZ_CP049363_-_outer_membrane_lipid_asymmetry_maintenance_protein_mlad	Extracellular	1	0,854	24,12	Insoluble	0.794
NZ_CP049363_-_hypothetical_protein 504	Extracellular	0	0,736	15,66	Soluble	0.826
NZ_CP049363_-_gsph/fimt_family_pseudopilin 2	Extracellular	1	0,628	16,84	Insoluble	0.887
NZ_CP049363_-_pilin	Extracellular	1	0,815	14,88	Insoluble	0.815
NZ_CP049363_-_omp33-36	Outermembrane	0	0,759	32,12	Insoluble	0.793
NZ_CP049363_-_putative_porin, pporin homolog	Outermembrane	0	0,669	27,65	Insoluble	0.660
NZ_CP049363_-_M23_family_metallopeptidase	Outermembrane	0	0,802	24,7	Insoluble	0.549

NZ_CP049363_-_TIGR04219_family_outer_membrane_beta-barrel_protein, omp homolog	Outermembrane	0	0,506	25,41	Insoluble	0.617

Table 4 – Immunogenicity prediction by MHCII binding prediction. SB – strong binding; WB – weak binding.

Protein	SB	WB	Total
NZ_CP049363_-_outer_membrane_beta-barrel_protein, ompw homolog	112	352	464
NZ_CP049363_-_hypothetical_protein 67	29	132	161
NZ_CP049363_-_OmpA_family_protein (OmpA2)	50	318	368
NZ_CP049363_-_bamE	56	222	278
NZ_CP049363_-_copper_resistance_protein_NlpE	8	23	31
NZ_CP049363_-_tetratricopeptide_repeat_protein 3	20	99	119
NZ_CP049363_-_hypothetical_protein 322	51	154	205
NZ_CP049363_-_porin	54	130	184
NZ_CP049363_-_type_VI_secretion_system_tube_protein_Hcp	11	39	50
NZ_CP049363_-_peptidoglycan_DD-metalloendopeptidase_family_protein 2	28	148	176
NZ_CP049363_-_pal	26	62	88
NZ_CP049363_-_Plug_domain-containing_protein	22	97	119
NZ_CP049363_-_OmpA-1_family_protein	43	126	169
NZ_CP049363_-_outer_membrane_lipid_asymmetry_maintenance_protein_MlaD	23	114	137
NZ_CP049363_-_hypothetical_protein 504	7	52	59
NZ_CP049363_-_GspH/FimT_family_pseudopilin 2	29	86	115
NZ_CP049363_-_pilin	17	57	74
NZ_CP049363_-_omp33-36	51	102	153
NZ_CP049363_-_putative_porin, pporin homolog	20	81	101

NZ_CP049363_-_M23_family_metallopeptidase	16	84	100
NZ_CP049363_-_TIGR04219_family_outer_membrane_beta-barrel_protein, omp homolog	22	105	127

Attachment II - Authorization to carry out animal experimentation

REPÚBLICA PORTUGUESA

AGRICULTURA

dgav
Direção Geral
de Alimentação
e Veterinária

Ex ᵐᵃ Senhora
Doutora Alexandra Fraga
Escola de Medicina da Universidade do Minho
Campus de Gualtar
4710 - 057 BRAGA

2021-11-19   018295

Nossa referência	Vossa referência	Vossa data
0421/000/000 /2021	Email	27/10/2021

Assunto: **PROTEÇÃO DOS ANIMAIS UTILIZADOS PARA FINS CIENTÍFICOS - PEDIDO DE PRORROGAÇÃO DE AUTORIZAÇÃO PARA REALIZAÇÃO DE PROJETO DE EXPERIMENTAÇÃO ANIMAL**

Na sequência do pedido efetuado por V. Exª no sentido de poder ser prorrogado o prazo da autorização para realização do projeto experimental designado "Utilização de fagos e endolisinas para o tratamento de doenças infecciosas", tendo por investigadores responsáveis os Professores Joana Azeredo e Jorge Pedrosa, cabe-me informar que o mesmo é **deferido**.

Assim sendo, a autorização em apreço emitida através do ofício nº 8421, de 11/4/2018, estender-se-á até **11/4/2022**.

Com os melhores cumprimentos,

A Diretora Geral

Susana Guedes Pombo

DBEA/APM

CAMPO GRANDE, Nº 50 1700-093 LISBOA TELEF. 21 323 95 00 FAX. 21 346 35 18

Attachment III. Endotoxin quantification

Figure showing the calibration curve plot with Optical Density on the y-axis (0.0 to 1.0) and EU / mL on the x-axis (0.0 to 1.5), with the equation $OD_{405nm} = 1.006 \times [EU] - 0.05$ and $R^2 = 0{,}9996$.
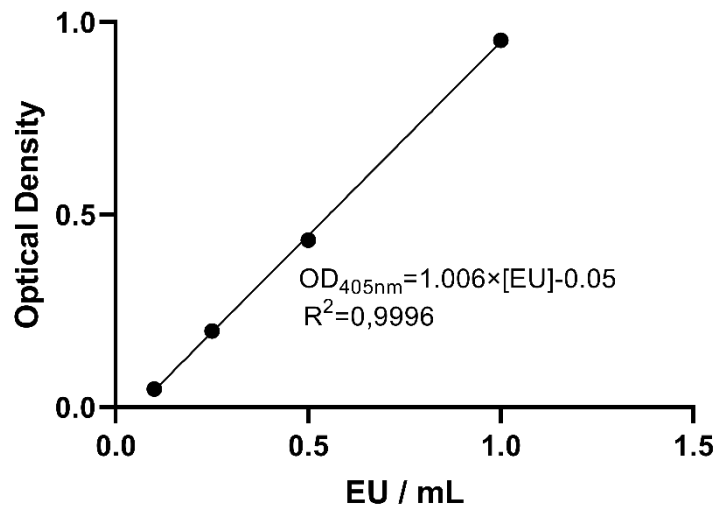
Figure 1 – Calibration curve. Calibration curve obtained through the linear regression of the values obtained. The calibration curve was obtained in order to extrapolate the equation used to calculate endotoxin values of samples.

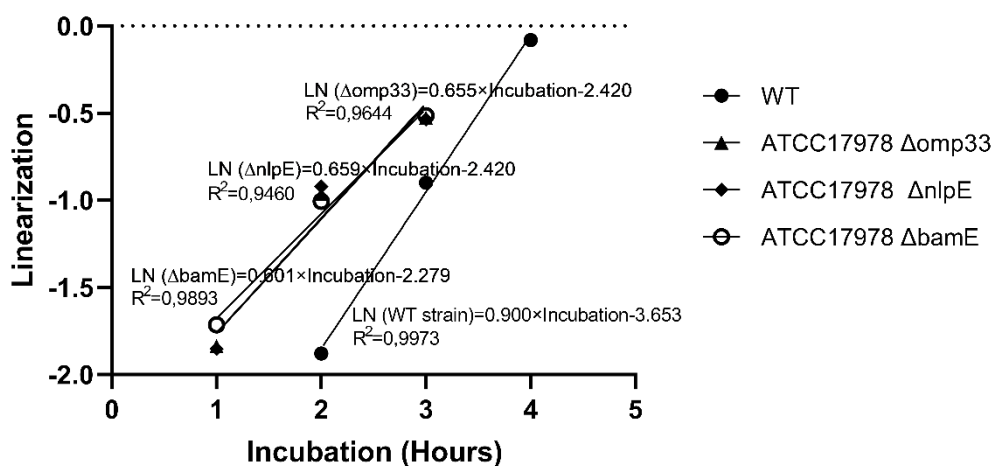# Attachment IV. Linearization of growth phases

Figure 1 – Linearization of exponential growth phases of the WT and mutants' strains. The exponential growth phase was delimited from the growth curves and the values linearized. Trough the linear regression shown, were extrapolated equation 2 to 5.

$$DT = \frac{ln(2)}{\mu} \quad \textbf{\textit{Equation 1}}$$

$$LN\ (WT\ strain) = 0.900 \times Incubation - 3.653 \quad \textbf{\textit{Equation 2}}$$

$$LN\ (\Delta omp33) = 0.655 \times Incubation - 2.420 \quad \textbf{\textit{Equation 3}}$$

$$LN\ (\Delta nlpE) = 0.659 \times Incubation - 2.420 \quad \textbf{\textit{Equation 4}}$$

$$LN\ (\Delta bamE) = 0.601 \times Incubation - 2.279 \quad \textbf{\textit{Equation 5}}$$

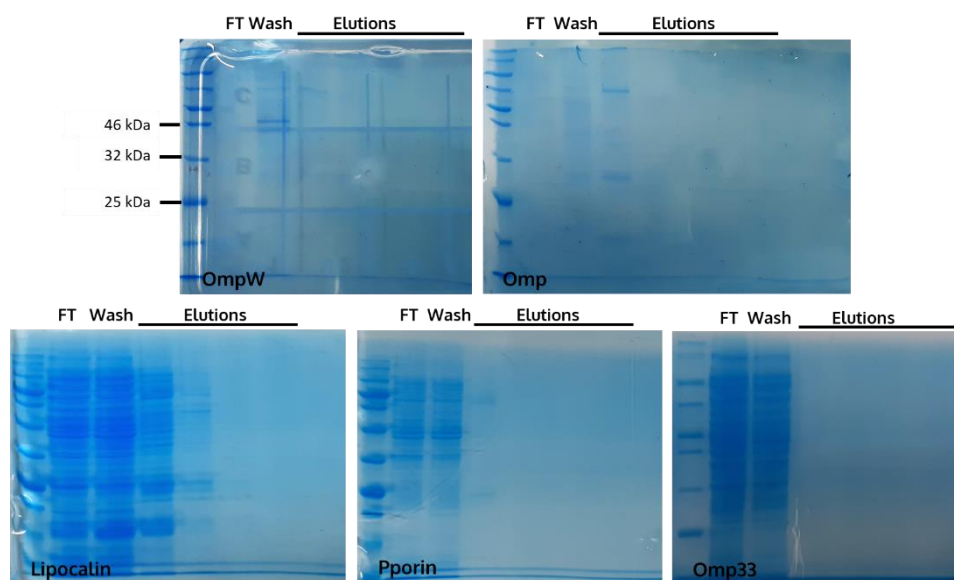# Attachment V. Protein Expression

Figure 1 – Unsuccessful expressions of proteins Omp, OmpW, Lipocalin, Pporin and Omp33 in _E. coli_ BL21 cells. 12% SDS-PAGE gels obtained from the expression of the proteins Omp, OmpW, Lipocalin, Pporin and Omp33 in _E. coli_ BL21. The ladder PageRuler Blue Prestained Protein Standard (New England BioLabs) was used.
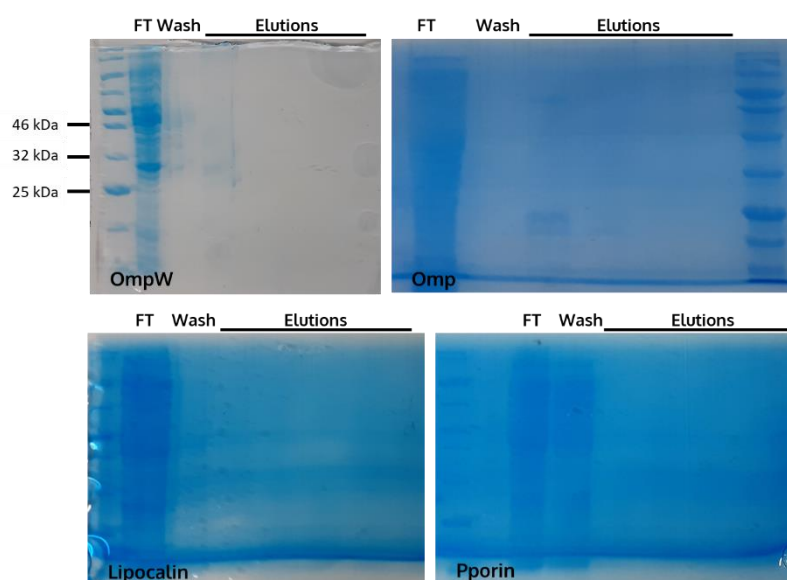

Figure 2 – Unsuccessful expressions of proteins Omp, OmpW, Lipocalin and Pporin in _E. coli_ C43 cells. 12% SDS-PAGE gels obtained from the expression of the proteins Omp, OmpW, Lipocalin and Pporin in _E. coli_ C43. The ladder PageRuler Blue Prestained Protein Standard (New England BioLabs) was used.
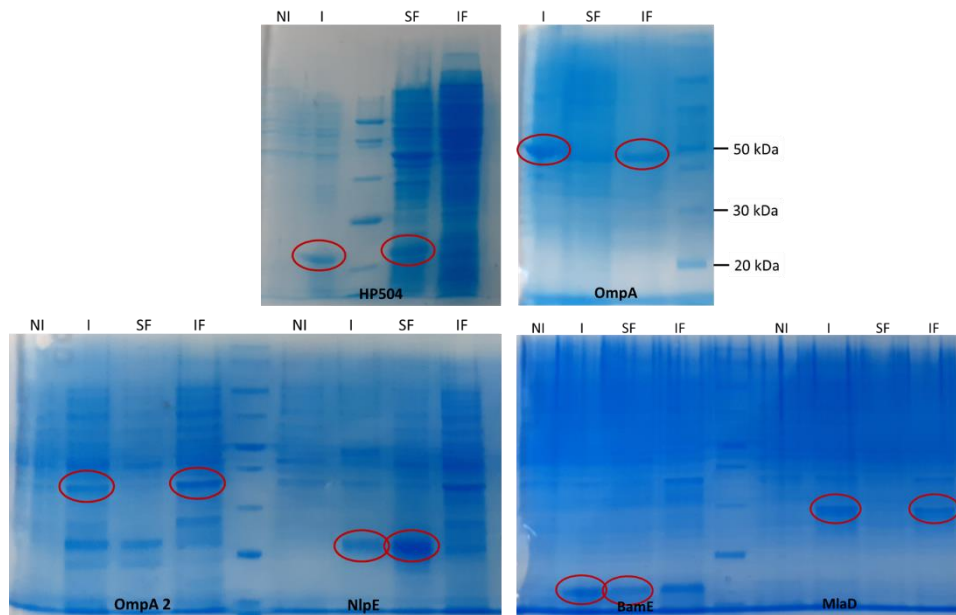
Figure 3 – Expression of proteins OmpA, OmpA2, NlpE, BamE, MlaD and HP504 without signal peptide. Proteins OmpA, OmpA2, NlpE, BamE, MlaD and HP504 were expressed without signal peptides to access if there would be overexpression of the proteins. Circled in red are the bands corresponding to each protein. The ladder PageRuler Unstained Broad Range Protein Ladder (Thermo Scientific) was used in all gels. NI – not induced; I – induced; SF – soluble fraction; IF – insoluble fraction.